

Recent advances and future perspectives of two-dimensional materials for rechargeable Li-O₂ batteries

Yajun Ding^{a,b}, Yuejiao Li^{a,e}, Min Wu^{a,c}, Hong Zhao^c, Qi Li^{b,d}, Zhong-Shuai Wu^{a,f,*}

^a State Key Laboratory of Catalysis, Dalian Institute of Chemical Physics, Chinese Academy of Sciences, 457 Zhongshan Road, Dalian 116023, China

^b Shenyang National Laboratory for Materials Science, Institute of Metal Research, Chinese Academy of Sciences, 72 Wenhua Road, Shenyang 110016, China

^c New Energy Laboratory, Dalian Jiaotong University, 794 Huanghe Road, Dalian 116028, China

^d School of Materials Science and Engineering, Southwest Jiaotong University, Chengdu 610031, China

^e University of Chinese Academy of Sciences, 19 A Yuquan Rd, Shijingshan District, Beijing 100049, China

^f Dalian National Laboratory for Clean Energy, Chinese Academy of Sciences, 457 Zhongshan Road, Dalian 116023, China



ARTICLE INFO

Keywords:

Li-O₂ batteries
2D Materials
Electrocatalysts
Cathode
Solid-state electrolytes
Dendrite-free anode

ABSTRACT

Li-O₂ batteries have drawn considerable interests owing to their highest theoretical energy density among the reported rechargeable batteries. However, Li-O₂ batteries are facing severe challenges in the low round-trip efficiency and poor cycling stability. Recently, two-dimensional (2D) materials with large surface area, tunable electrical/ionic conductivity, exceptional chemical and mechanical stability are emerging as a competitive candidate for Li-O₂ batteries. Herein, this review summarizes the key challenges and recent advances of 2D materials, serving as multi-functional roles in the design of advanced cathodes, development of solid-state electrolytes and separators, and protection of lithium anodes for high-energy-density nonaqueous Li-O₂ batteries. Firstly, the current status is introduced to highlight the significance and bottlenecks of Li-O₂ batteries. Second, the state-of-the-art 2D materials are exemplified to illustrate their key roles in cathodes, electrolytes, separators and anodes. Specifically, 2D materials with high electrical conductivity, hierarchically porous structure and enriched functionalities are very promising for design of ideal cathodes that can significantly facilitate the transfer of electrons and mass, offer enough accommodation space for discharge products. Moreover, 2D materials modified separators and solid-state electrolytes with superionic conduction and outstanding stability can greatly boost ionic mobility and prolong the cycling life. Besides, nanostructure engineering of stable solid electrolyte interface film and Li metal anode using 2D materials as coating layers and lithophilic hosts with high chemical stability and mechanical strength can effectively suppress the growth of Li dendrites during plating/stripping. Finally, the future challenges and development directions of Li-O₂ batteries based on advanced 2D materials are briefly discussed.

1. Introduction

With the ever-increasing global energy crisis caused by shortage of fossil fuels and serious environmental issues, the whole world is making great efforts to develop the inexhaustible renewable energy (e.g., solar, ocean energy) and their energy storage systems, in which electrochemical energy storage and conversion technologies have attracted enormously attentions due to their high efficiency, accessibility and compatibility for environment, such as fuel cells [1,2], metal-ion batteries [3,4], metal-air batteries [5,6] and supercapacitors [7,8]. As we known, Li-ion batteries are the most concerned and commercially available batteries, but approaching their theoretical energy density. To meet urgent requirement of long-range electrical vehicles and portable electronic devices [9–12], it is imperative to advance rechargeable batteries with higher energy density, such as rechargeable Li-O₂ batteries, due to the

highest energy density (11,700 Wh kg⁻¹ based on Li-metal mass) in theory compared with any other rechargeable batteries (Fig. 1a) [13–15].

In principle, Li-O₂ battery is consisted of Li metal anode, electrolyte, separator and oxygen cathode. The interconversion between electric and chemical energy realizes through reversible reactions between lithium oxides and Li metal at anode, oxygen at cathode, respectively [12,16–18]. As the reactant O₂ at cathode comes from the ambient air instead of being placed inside the batteries, Li-O₂ batteries are also called Li-air batteries. Generally, Li-O₂ batteries are classified into four types according to the employed electrolytes: (1) aqueous, (2) aprotic, (3) solid-state, and (4) hybrid systems (Fig. 1b) [19,20]. Although the open circuit voltages of aqueous Li-O₂ batteries are higher (3.44 and 4.27 V in basic and acidic electrolytes, respectively) than that of aprotic Li-O₂ batteries (2.96 V), the aqueous systems gradually fails to attract sustained attention because of the side reaction on vulnerable Li metal when con-

* Corresponding author.

E-mail address: wuzs@dicp.ac.cn (Z.-S. Wu).

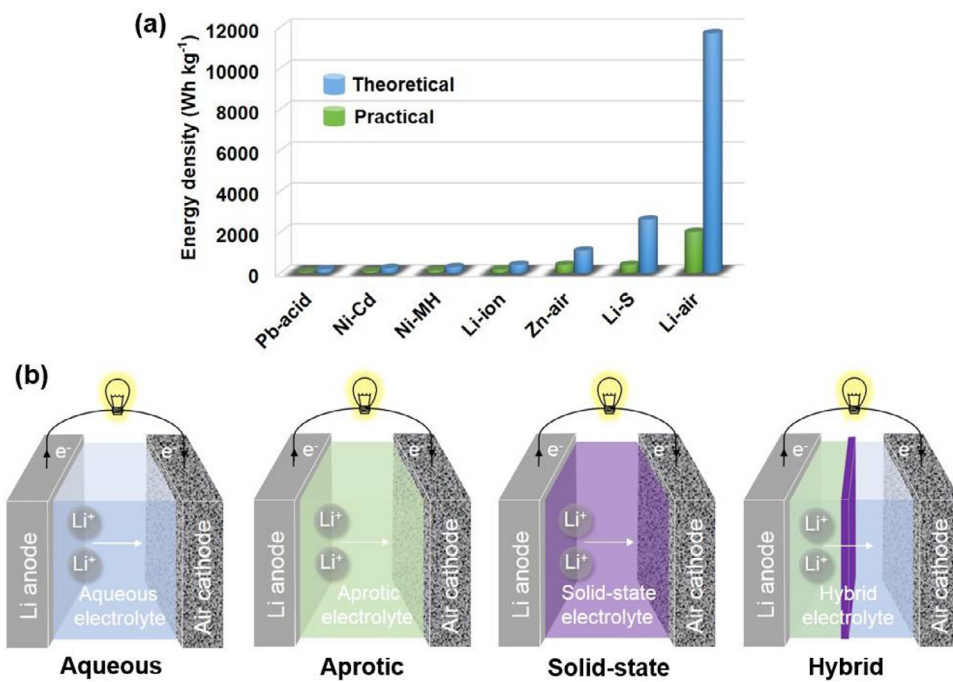


Fig. 1. (a) Gravimetric energy densities values of the representative batteries: Pb-acid, Ni-Cd, Ni-metal hydride (Ni-MH), Li-ion, Zn-air, Li-S and Li-air batteries. Theoretical values of metal-air batteries are achieved on basis of relative metal mass. (b) Schematic of the four types of Li-O₂ batteries.

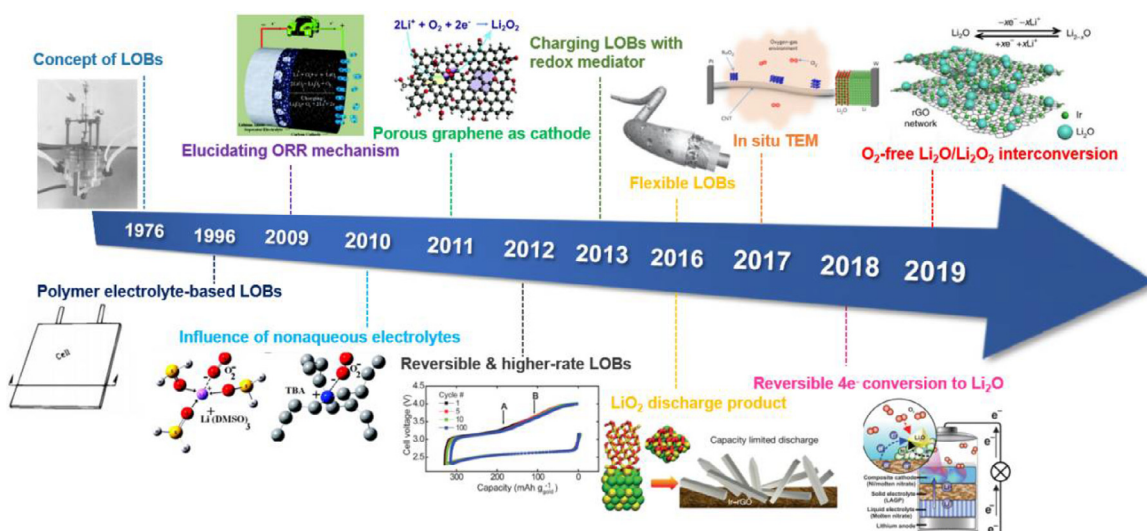


Fig. 2. Selected major events of Li-O₂ batteries (LOBs) from 1976 to 2019. 1976: The concept of LOBs. Reproduced with permission from Ref. [25], Copyright 1976, The Electrochemical Society. 1996: Polymer electrolyte-based LOBs. Reproduced with permission from Ref. [26], Copyright 1996, The Electrochemical Society. 2009: Elucidating ORR mechanism. Reproduced with permission from Ref. [27], Copyright 2009, American Chemical Society. 2010: Influence of nonaqueous electrolytes. Reproduced with permission from Ref. [28], Copyright 2010, American Chemical Society. 2011: Porous graphene as cathode. Reproduced with permission from Ref. [29], Copyright 2011, American Chemical Society. 2012: Reversible & higher-rate LOBs. Reproduced with permission from Ref. [30], Copyright 2012, American Association for the Advancement of Science. 2013: Charging LOBs with redox mediator. Reproduced with permission from Ref. [31], Copyright 2013, Nature Publishing Group. 2016: Flexible LOBs [32], and LiO₂ discharge product [33]. Reproduced with permission from Refs. [32,33], Copyright 2016, Wiley-VCH and Nature Publishing Group. 2017: *In situ* transmission electron microscopy (TEM). Reproduced with permission from Ref. [34], Copyright 2017, Nature Publishing Group. 2018: Reversible 4e⁻ conversion to Li₂O. Reproduced with permission from Ref. [35], Copyright 2018, American Association for the Advancement of Science. 2019: O₂-free Li₂O/Li₂O₂ interconversion. Reproduced with permission from Ref. [36], Copyright 2019, Nature Publishing Group.

tacting with aqueous electrolytes [19,21–23]. In contrast, nonaqueous Li-O₂ batteries could offer higher energy density and rechargeability, which have gained enormous attention (Fig. 2) [14,24]. Therefore, this review will mainly centralize on the recent advances of the nonaqueous system of Li-O₂ batteries.

In the pioneering work, Littauer and Tsai firstly put forward the concept of aqueous Li-O₂ batteries in 1976 [25,37], and then Abraham and Jiang developed the solid-state Li-O₂ batteries in 1996 [26]. Despite of high theoretic energy density, Li-O₂ batteries were fell out of favor due to the seemingly insuperable barrier between theory and reality. Later, nonaqueous Li-O₂ batteries recaptured scientific attention recently be-

cause of achievable higher energy density than those of the reported previously. For example, Bruce et al. developed a Li-O₂ battery with dimethyl sulfoxide as the electrolyte and nanoporous gold cathode cycling via the formation of Li₂O₂, which delivered excellent reversibility and rate capability [30]. In contrast to the Li₂O₂-based Li-O₂ battery, gray et al. creatively designed a rechargeable Li-O₂ battery cycling through LiOH formation and decomposition at cathode, which can tolerate high concentrations of water [38]. Different from the previous studies in view of discharge products, Lu et al. constructed a novel Li-O₂ cell based on LiO₂ as the discharge products through one-electron discharge process [33]. However, both Li₂O₂ and LiO₂ react with organic electrolytes and carbon in the cell. In order to explore more stable discharge products, Nazar et al. developed a high capacity (11 mAh cm⁻²) Li-O₂ batteries based on discharge product of Li₂O [35]. Though these exciting advances highlighting the importance of Li-O₂ cells, there are still significant challenges remained, e.g., (i) low round-trip efficiency, specific capacity and rate capability caused by poor activity of the catalyst and non-ideal structure of cathode; (ii) short cycling-life caused by unstable electrolyte; and (iii) safety issues resulting from improper separator and formation of Li dendrites [19,24,39,40]. To solve gordian issues, advancing the materials employed in each part of batteries plays a critical role in developing Li-O₂ batteries.

Recently, two-dimensional (2D) materials have drawn increasing interests to enhance the performance of Li-O₂ batteries due to their unique architectures, which could efficiently settle various problems of cathode, solid-state electrolyte, separator and anode in Li-O₂ batteries [41–44]. Generally, the controllable structure, ultrathin thickness, electrical/thermal/ionic conductivity, hydrophilicity/hydrophobicity, and defect sites of 2D materials play a crucial part in their applications for Li-O₂ batteries [45]. Specifically, high surface area and enriched functionality of 2D materials can boost electrocatalytic reaction and thus lower overpotential during discharge and charge process, which promotes the round-trip efficiency for Li-O₂ batteries. More significantly, 2D materials with hierarchically porous structure, e.g., 3D assembled networks, can substantially accommodate more discharge products for enhanced energy density. Moreover, the superior electrical/ionic conductivity of 2D materials can lower the ion and/or electron mobility barriers to facilitate fast surface/interface redox reactions, and their band gap tunable properties provide intriguing opportunities from cathode and anode to separator and solid-state electrolyte when they are tuned to highly electrical insulator [41,46–48]. Therefore, Li metal dendrite formation and propagation could be efficiently suppressed by coating appropriate 2D materials with chemical and mechanical stability on separators and/or anode [46,49], resulting in prolong cycle life for Li-O₂ batteries [50]. Finally, 2D materials are the highly suitable candidates for flexible Li-O₂ batteries with endurance for high stress and strain [51]. In short, 2D materials with outstanding properties have exhibited considerable improvement and promising prospects for rechargeable Li-O₂ cells.

In this review, we summarize the current advances of 2D materials for rechargeable Li-O₂ batteries, and highlight the key roles of 2D materials on how to address the main challenges in the cathode, electrolyte, separator and anode in nonaqueous Li-O₂ batteries. Firstly, we briefly introduce the main bottlenecks of Li-O₂ batteries for the commercialization based on the cathode, nonaqueous electrolyte, separator and anode. Then, the promising solutions for these bottlenecks in major parts of Li-O₂ cells are elaborately discussed based on 2D materials. Specifically, 2D materials based cathodes with large surface area, hierarchical porous structure and excellent electrical conductivity could efficiently improve the energy density and increase round-trip efficiency, implemented by doping, defect engineering, functionalization and assembly design. Moreover, 2D materials with high ionic conductivity and electrical insulating are good additives of separator and solid-state electrolyte to increase the rate capacity and prolong cycling life for nonaqueous Li-O₂ cells. Meanwhile, 2D materials with outstanding mechanical and chemical stability could sufficiently prevent the anode from pulverization, side reactions and dendrites, leading to high capacity and safety.

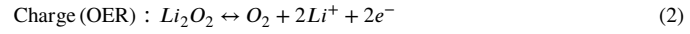
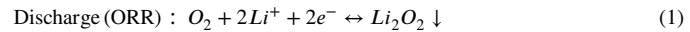
Finally, the future perspectives and possible research directions of 2D materials for rechargeable Li-O₂ cells are briefly discussed in the last section.

2. Overview of the challenges for Li-O₂ batteries

The major challenges in terms of the key materials in Li-O₂ batteries can be classified based on different components of cathode, nonaqueous electrolyte, separator and anode.

2.1. Cathode

Numerous studies have intensively concerned the core part of Li-O₂ batteries, cathode, especially the oxygen electrocatalysts and electrode structure [19,52–54]. Generally, the O₂ from outside environment is considered to be reduced to lithium oxides during discharge process (oxygen reduction reaction, ORR), while the formed lithium oxides can be reversibly decomposed to O₂ through charge process (oxygen evolution reaction, OER) [55]. The discharge products vary from LiO₂, Li₂O₂, Li₂O, LiOH to other byproducts (such as Li₂CO₃) caused by the disparity of used electrocatalysts, electrode structure and electrolytes [24,30,33,35,38]. However, it is hard to evaluate which type of discharge products is desirable because the complexity and standardization of Li-O₂ batteries are not well established. Usually, Li₂O₂ is considered as an ideal discharge product due to its high electrochemical reversibility [53,56]. On basis of Li₂O₂ as discharge product, it is generally accepted that the ORR/OER reactions of Li-O₂ cells at cathode are described as the Eqs. (1) and (2):



Even though the 2e⁻ electrochemical reactions in nonaqueous electrolyte are considered to occur more easily than 4e⁻ process in aqueous electrolyte, there are still a large amount of issues derived from materials optimization. The sluggish kinetics and rapid deterioration for the OER and ORR are originating from the lacking of matched active sites and 3D interconnected structure of electrocatalysts, resulting in the large polarization during charging and discharging and low round-trip efficiency [19]. In particular, the continuous deposition of insulating and insoluble Li₂O₂ undoubtedly blocks the electron transfer and oxygen diffusion channels upon cycling, leading to the broken batteries [54]. Furthermore, the conventional structure of electrodes could not provide rational pathway for fast mass/electron transfer and large storage space for discharge products [57]. Besides, the catalysts could not offer the optimized distribution, morphology and produce the desirable type of discharge products. Consequently, the Li-O₂ batteries usually perform low capacity and short lifetime [20].

Tremendous efforts have been made to settle these cathode issues from the perspective of materials. For example, Hu et al. fabricated a flexible wood (F-Wood) cathodic material with tri-pathway from balsa wood (Fig. 3) [58]. Inspired by multiphase transport in tree, they creatively designed this tri-pathway wood-based cathode for ions, O₂ and electrons, which showed large discharge capacity (67.2 mAh cm⁻²) and long cycling stability (220 cycles). It is worth noting that this nature-inspired design developed a novel and general method for the construction of energy storage devices carried out by multiphase transport. Similarly, an open-structured Co₉S₈ cathode reported by Dong et al. provided highly active sites for oxygen redox reactions, efficient contact interface between cathode and Li₂O₂, and efficient storage space for discharge products (Fig. 4a-i). As a result, this porous carbon foil (PCF) supported Co₉S₈ catalyst exhibited a very small overpotential of 0.57 V under 1000 mA g⁻¹ and a moderate discharge capacity of 6875 mAh g⁻¹ under 50 mA g⁻¹ [59]. Therefore, the design principle of cathode materials should take several aspects into account, such as active

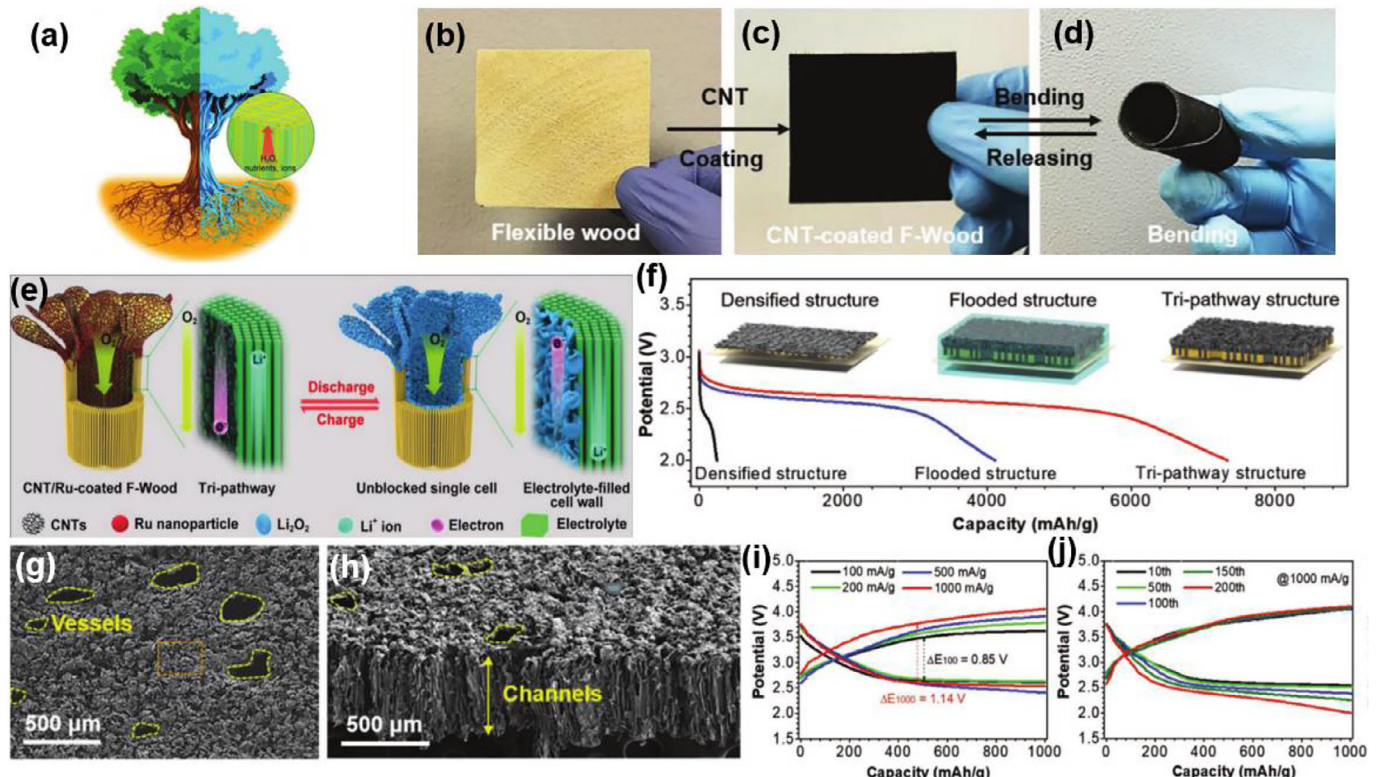


Fig. 3. (a) Multiphase transport in trees. (b-d) Photographs of (b) F-Wood, (c) as-prepared and (d) bent CNT-coated F-Wood. (e) Schematic of the breathable Li-O₂ batteries with CNT/Ru-coated F-Wood-based cathode. (f) Discharge plots of the 1st cycle for CNT/Ru-coated F-Wood-based cathode with various amount of electrolyte. (g,h) Scanning electron microscopy (SEM) images of CNT/Ru-coated F-Wood films: (g) top and (h) cross-sectional view. (i) Charge-discharge plots obtained at various current densities. (j) Charge-discharge curves at 1000 mA g⁻¹. Reproduced with permission from Ref. [58], Copyright 2019, Wiley-VCH.

phases to accelerate the ORR/OER, and abundant porous structure to store discharge products. Besides, the formation/evolution ways of discharge products can also affect the capacity, cycle life and overpotentials of discharge/charge. For example, Shahbazian-Yassar et al. employed the MnO₂ cathode catalysts with different lattice facets to modulate the formation routes of discharge products Li₂O₂. Importantly, they found rational facet engineering of MnO₂ crystals could efficiently reduce the charge overpotential (0.89 V) and discharge overpotential (0.3 V) in comparison to bare carbon counterpart. Specifically, β -MnO₂ with {111} facets catalyzed the solution mechanism forming Li₂O₂ toroids, while the {100} facets facilitated the surface mechanism to generate Li₂O₂ films (Fig. 4j, k) [60]. Constructing rational oxygen cathodes with superior active and uniformly dispersed electrocatalysts is another effective approach to decrease the overpotentials during charge and discharge process. As an example, Sun et al. developed Mn₃O₄/CNTs-RuO₂ film as Li-O₂ cell cathode by depositing RuO₂ nanoparticles on self-assembled Mn₃O₄ nanowires and CNTs composite, delivering a remarkable round-trip efficiency (83%) and outstanding cycle stability (251 cycles) reported to date [61].

Ideally, the high-performance cathode materials should be simultaneously equipped with uniformly dispersed active sites and superior dual-functional electrocatalytic activity toward ORR/OER, highly electrical conductivity, outstanding chemical and mechanical stability, and optimized hierarchically porous structure that not only store discharge products as much as possible but also possess rapid diffusion pathway of electrolyte and oxygen.

2.2. Nonaqueous electrolyte

Nonaqueous electrolytes include aprotic electrolyte and quasi/all-solid-state electrolyte. So far, the aprotic electrolytes have been inten-

sively studied in Li-O₂ cells [62–66]. Nevertheless, they suffer from easy decomposition and volatilization, low conductivity, oxygen solubility, donor number and high viscosity, especially the frequency side reaction with Li anode, oxygen and intermediate species [41,67,68]. Conversely, the quasi/all-solid-state electrolytes show more promising owing to the advantages compared with aprotic counterpart [69–72]. They are not prone to the volatilization, leakage or other side reactions. In addition, other issues, such as Li dendrite growth, internal shorting, corrosion of lithium metal by H₂O, CO₂ and O₂ species, could be efficiently suppressed owing to the intrinsic solid characteristics of solid-state electrolytes [73].

The reported solid-state electrolytes can be classified into organic (polymer) and inorganic (ceramic) electrolytes. Recently, Zhou et al. have systematically summarized the advancement of polymer electrolytes in solid-state Li-O₂ cells [74], and highlighted that polymer electrolyte would be a better candidate than ceramic electrolyte as the alternative of liquid electrolytes due to their outstanding processability and mechanical strength. In fact, the study on the solid-state Li-O₂ batteries is still in the early phase now. Although some advancements of solid-state electrolytes have been achieved, there are still various challenges, such as the low ionic conductivity, poor diffusion properties for polymer electrolytes, and frangibility for ceramic electrolytes [75–77]. To develop high ionic conductive and flexible solid-state electrolyte with simultaneously, the hybrids solid-state electrolyte combining superior compatibility, flexibility of polymer and highly ionic conductivity, chemical stability of ceramic materials should be a better choice.

2.3. Separator

The role of separator employed in nonaqueous Li-O₂ batteries is mainly to prevent electron, oxygen, reactive oxygen species and other

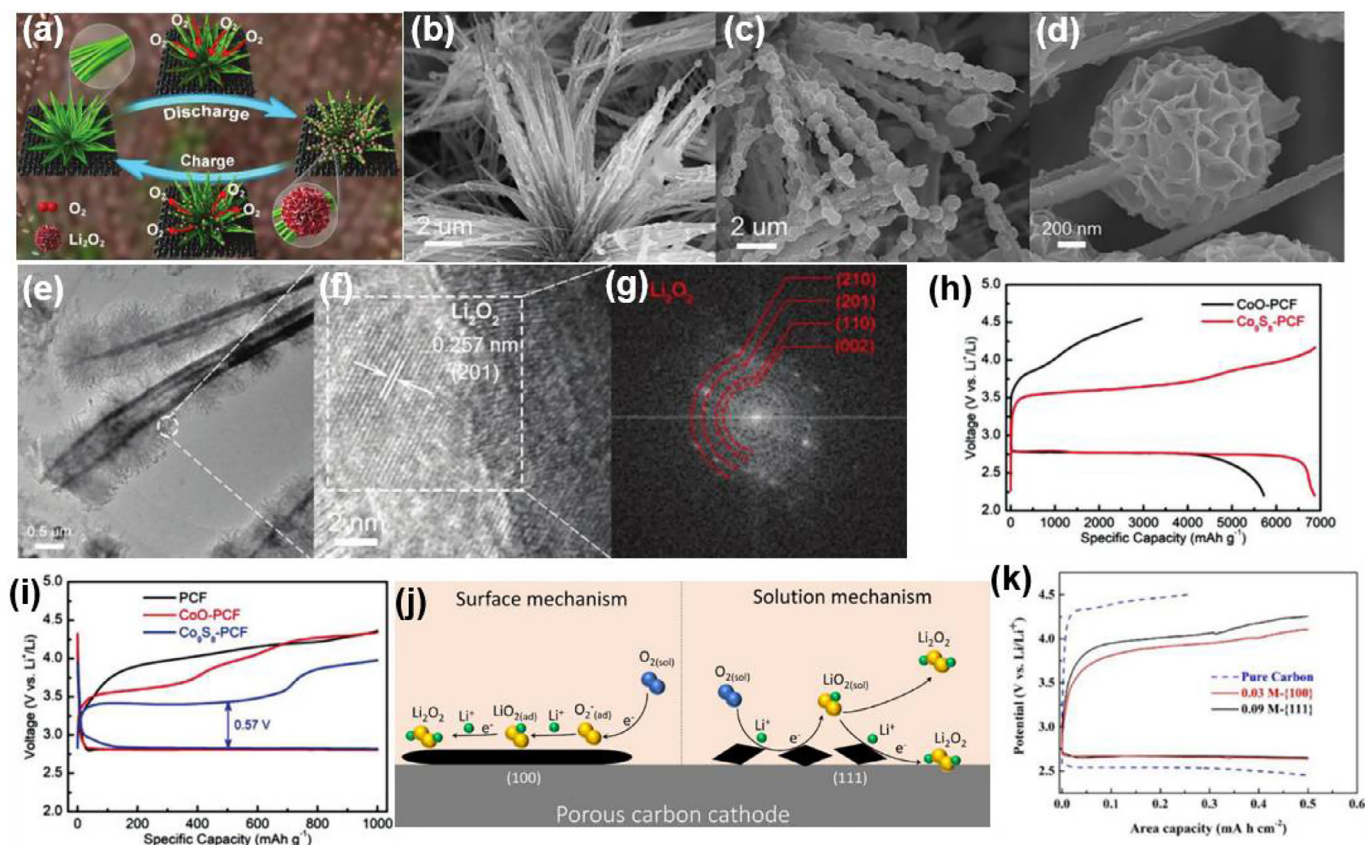


Fig. 4. (a) Schematic of constructing Co₉S₈-PCF cathode. (b-d) SEM image of (b) half and (c,d) complete discharged Co₉S₈-PCF. (e) TEM, (f) HRTEM and (g) FFT images of Co₉S₈-PCF cathode discharged. (h) Discharge and charge plots with PCF, CoO-PCF, and Co₉S₈-PCF cathodes at 50 mA g⁻¹ and 1000 mAh g⁻¹. (i) Full discharge and charge plots with CoO-PCF and Co₉S₈-PCF cathodes at 50 mA g⁻¹. Reproduced with permission from Ref. [59], Copyright 2018, Wiley-VCH. (j) Possible Li₂O₂ formation mechanisms catalyzed by β -MnO₂ with {100} and {111} facets. (k) The 1st cycle charge-discharge plots of the Li-O₂ batteries based on β -MnO₂ with {100} and {111}. Reproduced with permission from Ref. [60], Copyright 2019, American Chemical Society.

intermediate reactants from the permeation between cathode and anode [78–80]. Certainly, the solid-state electrolyte can play the role in separator, but this separator is usually out of full consideration for solid-state Li-O₂ batteries. In the previous works, various ceramic and organic materials were proposed to modify the boughten separator, enhancing its performance in Li-O₂ cells [81–83]. For instance, Hu et al. fabricated a boron nitride (BN) nanosheets coated separator to inhibit the Li dendrite growth [80]. Notably, the usages of BN-coated separator in aprotic electrolyte resulted in a stable coulombic efficiency of 92% for >100 cycles at 0.5 mA cm⁻² and 88% at 1.0 mA cm⁻². Moreover, Hammond et al. fabricated an excellent separator by depositing an ionic conductive polymer and graphene oxide (GO) on a polymer support membrane [84], which possessed controlled electrolyte permeability of 1.42×10^{-12} m², superionic conduction of 0.29 mS cm⁻¹ and Li transfer number of 0.52, thus resulting in the suppression of Li dendrites for superior cyclability of 281.1 h.

However, there are only a few of experimental studies on separator for Li-O₂ batteries, and many challenging issues remind unsolved. Specifically, poor mechanical/thermal properties are the main hindrances of organic separators, while high thickness, frangibility and nonuniform porosity are the key bottlenecks of inorganic separators.

2.4. Anode

Li metal anode has drawn increasingly interests owing to the considerably large gravimetric capacity of 3860 mAh g⁻¹ in theory, low negative redox voltage of -3.04 V (vs. SHE) and mass density of 0.59 g cm⁻³ [85–88]. Therefore, Li metal anode is widely acknowledged as the

most hopeful anode for rechargeable cells, e.g., Li-O₂ cells, with large specific energy of 11,700 Wh kg⁻¹ in theory [89,90]. Unfortunately, Li metal anode of rechargeable batteries has two knotty issues. On one hand, the isolated and continuous formation of Li dendrites caused by irreversible deposition of Li results in so-called “dead Li” and/or piercing of separator, which consequently lead to the decrease of capacity, cycling life and short circuit [91,92]. One the other hand, the highly reactive Li metal likely induces a series of side reactions with unstable electrolyte and cross-over O₂, H₂O, and CO₂ [26,93,94]. Therefore, it is significantly urgent to address these challenges for Li anodes promoting overall performance of Li metal batteries.

In this regard, there are four main technologies on suppressing Li dendrites via tuning surface energy of the Li metal anode, including an artificially prepared “hard film”, a solid electrolyte interface (SEI) film formed from reacting with other materials, the additives introduction into the electrolytes for retarding the growth of Li dendrites, and nanostructure materials coated on the anode for guiding the growth of Li dendrites along the direction of nanostructure [40]. Inspired by the protection function of the umbrella, Zhang et al. reported a hydrophobic hybrids polymer electrolyte film with high stability, hydrophobicity and flexibility to protect the Li metal anode. As a result, this protective strategy greatly prolonged the cycling life of Li-O₂ batteries from 24 cycles to 95 cycles [95]. Moreover, Peng et al. employed cross-stacked aligned carbon nanotube sheets on the Li metal anodes to achieve high reversible specific capacity of 3656 mAh g⁻¹ that approached the pure Li value in theory [96]. Although these advances for protecting Li anode, the issue of Li dendrites still perplexes the researchers for applying the Li metal electrode into the real cell, espe-

cially the rechargeable Li-O₂ batteries working under tougher operating condition.

3. Advances of 2D materials for Li-O₂ batteries

As discussed above, the development of rechargeable Li-O₂ batteries is facing great challenges, which can be efficiently addressed by choosing and designing suitable materials in major parts of batteries. 2D materials possess the capability of overcoming these issues due to their abundant merits for Li-O₂ batteries. To facilitate the study in Li-O₂ cells, the advanced 2D materials employed as cathode, solid-state electrolyte, separator and anode, respectively, for nonaqueous Li-O₂ cells will be elaborated in this section, and the corresponding key roles of 2D materials on the excellent performance of nonaqueous Li-O₂ cells will be summarized concretely as following section.

3.1. 2D materials for cathode

Cathode materials are the most investigated part of Li-O₂ batteries over past decades but still remain challenging [19,20,56,97]. To address this, 2D materials could provide large specific surface areas with abundant active sites and highly electrical conductivity, which are superior to their bulk counterparts [43,45]. Briefly, 2D materials can not only act as the oxygen electrocatalysts, but also serve as the support of cathodic catalysts. Generally, the role of 2D electrocatalyst is to provide the active sites for ORR and OER, and thus decrease the overpotential of these sluggish reactions in kinetics [16]. The optimized cathode matrix of 2D materials with rational structure is used to furnish multi-pathways for the electron, electrolyte, O₂ and storage space for discharge products [58]. To clearly specify the roles, we will catalog these 2D materials into four groups, including (i) graphene-based materials, (ii) transition metal oxides (TMOs)/transition metal hydroxides (TMHs), (iii) transition metal chalcogenides (TMCs), and (iv) other 2D materials based on the different elements and components for the cathodes of Li-O₂ batteries.

3.1.1. Graphene-based materials

Graphene and its derivatives have been studied most widely in nonaqueous Li-O₂ batteries. This is because graphene possesses an extraordinarily large specific surface area of 2630 m² g⁻¹, highly intrinsic charge carrier mobility up to 2.5 × 10⁵ cm² V⁻¹ g⁻¹ and extremely high Young's modulus up to 1 TPa. The chemically inert property results from homogeneous sp² hybridized electron distribution allows graphene to act as excellent 2D supports of ORR/OER catalysts [98–101]. Although the pure sp²-bonded plane of graphene is considered to be completely impermeable to all gasses and liquids, the defective graphene, e.g., activated graphene, holey graphene, porous graphene, derived from graphene oxide opens many opportunities for the design of suitable cathodes of Li-O₂ battery systems [102–104].

Notably, graphene is widely explored as efficient electrocatalysts for ORR and/or OER [105,106]. Considering the inert nature of pure graphene, introduction of the defective sites, single or multiple heteroatoms such as B, N, O, S or P into graphene can break the electric neutrality in the basal plane of graphene, and produce chemically active materials [107,108]. For example, Wu et al. synthesized a N-doped graphene composite catalyst by graphitization of a heteroatom polymer. Compared to the commercial carbon blacks and Pt/C catalysts [109], this graphene-based electrocatalyst delivered steadily improved activity towards ORR/OER in nonaqueous Li-O₂ cell due to high level of quaternary, pyridinic N (> 8 at% in total) and graphene-sheet-like structure. Further, Xiao et al. prepared a graphene-based cathode material prepared with a novel bimodal porous structural and functionalized graphene, which exhibited large discharge capacity of 15,000 mAh g⁻¹ at 0.1 mA cm⁻². It is considered that the oxygen could diffuse promptly in the micropores of this hierarchically porous graphene, and especially highly connected functional groups and defects in nanoscale

on graphene could provide abundant active sites for Li-O₂ battery reaction, which could greatly promote the deposition of isolated Li₂O₂ to keep O₂ from being blocked in the cathode [29].

Despite of the advances of bare graphene materials, their relatively sluggish kinetics of ORR/OER could hardly afford multi-functional requirements of cathodes in Li-O₂ batteries. To this purpose, anchoring noble metal and metal compounds on functional graphene with enriched reactive sites for ORR and OER became a promising alternative way to promote the performance of Li-O₂ cells [2,5,110]. Typically, Lu et al. synthesized the Ir-rGO electrocatalyst for Li-O₂ battery (Fig. 5), and showed that the formed LiO₂ product was stable to be reversibly recharged at potential down to 3.2 V, guaranteeing high-energy-density for Li-O₂ cells. Interestingly, Ir₃Li intermetallic compounds on the large Ir particles have a similar crystallographic lattice to that of LiO₂, acting as a template for growth of the crystalline LiO₂ [33]. Furthermore, Lee et al. fabricated rGO loaded Ru-based nanoparticles as cathode of Li-O₂ batteries [111], in which metallic Ru or RuO₂·0.64H₂O nanoparticles (< 2.5 nm) were homogeneously dispersed on rGO, and thus efficiently electrocatalyzed the LiO₂ oxidation reactions and stably run for 30 cycles. Especially, RuO₂·0.64H₂O-rGO hybrids exhibited superior activity to Ru-rGO hybrids and excellent stability without LiOH detected due to the structural water in the molecular structure of hydrated RuO₂. Similarly, completely hexagonal Ru quantum dots uniformly supported on N-doped graphene was reported by Kang et al. as an OER catalyst for Li-O₂ battery, exhibiting lower charge overpotentials of ~0.64 V than that of the bare N-doped holey graphene (~1.54 V) [112]. In addition, Liao et al. systematically examined the PdM (M = Fe, Co, Ni) alloys with face-centered cubic (fcc) phase structure on N-doped reduced graphene oxide (N-rGO) as the bifunctional ORR/OER catalyst [113]. It is noted that, among these catalysts, PdFe/N-rGO exhibited the most durable stability of 400 cycles under 1000 mAh g⁻¹ and 400 mA g⁻¹ due to the easier metal (Co and Ni) dissolution during cell cycling operation. In spite of outstanding performance of precious metal-based catalysts, the high cost and scarcity of these precious catalysts would substantially hinder their large-scale implementation.

To this end, non-noble metals or metal oxides hybridized with graphene were developed as electrocatalysts in nonaqueous Li-O₂ cells. For instance, Bao et al. developed a N-doped graphene shell with single layer encapsulated non-noble metal Co served as an outstanding OER electrocatalyst in nonaqueous Li-O₂ cells [114], which reached up to 90 cycles under 200 mA g⁻¹ and cutoff capacity of 600 mAh g⁻¹. Theoretically, it is uncoiled that Co clusters and N dopant could synergistically tune electrical structure of the supports to change the thermodynamic free energies of the intermediates, leading to a low charge overpotential of 0.58 V. In view of ORR, Kumar et al. prepared the self-assembled Ni anchored rGO with wrinkle structure hybrids by *in situ* reduction method [115], in which the synergistic improvement in the performance between Ni and rGO for ORR was demonstrated in nonaqueous electrolyte. Further, Tour et al. revealed that the cathode materials of MnNiFe/laser-induced graphene in Li-air battery [116] could stabilize the operation over 300 cycles at 0.4 mAh cm⁻² and deliver the discharge capacity of 26.3 mAh cm⁻². Moreover, Kim et al. reported a porous CuO/graphene hybrid obtained by coupling a porous 1D monoclinic CuO with graphene [117], which exhibited higher reversibility with a lower potential gap of 1.39 V than that of graphene catalyst during 120 cycles at 1000 mAh g⁻¹. Later, this group also proposed a bifunctional 1D/2D composite catalyst composed of Co₃O₄ nanofibers (NF) anchored on two sides of non-oxidized graphene nanoflakes (GNF) with hexagonal structure as superior oxygen electrocatalyst in ORR/OER for Li-O₂ cells [118], achieving large discharge capacity up to 10,500 mAh g⁻¹ and excellent cycle stability of 80 cycles under 1000 mAh g⁻¹ (Fig. 6a-g). Based on this concept, a 1D/2D CuGeO₃-graphene (CuGeO₃-G) composite with a sheet-like morphology was sequentially developed to synergistically enhance the ORR/OER bifunctional performance in aprotic Li-O₂ cells [119]. As expected, the well-designed CuGeO₃-G composite displayed superior bifunctionally electrocatalytic behavior with low Tafel slope

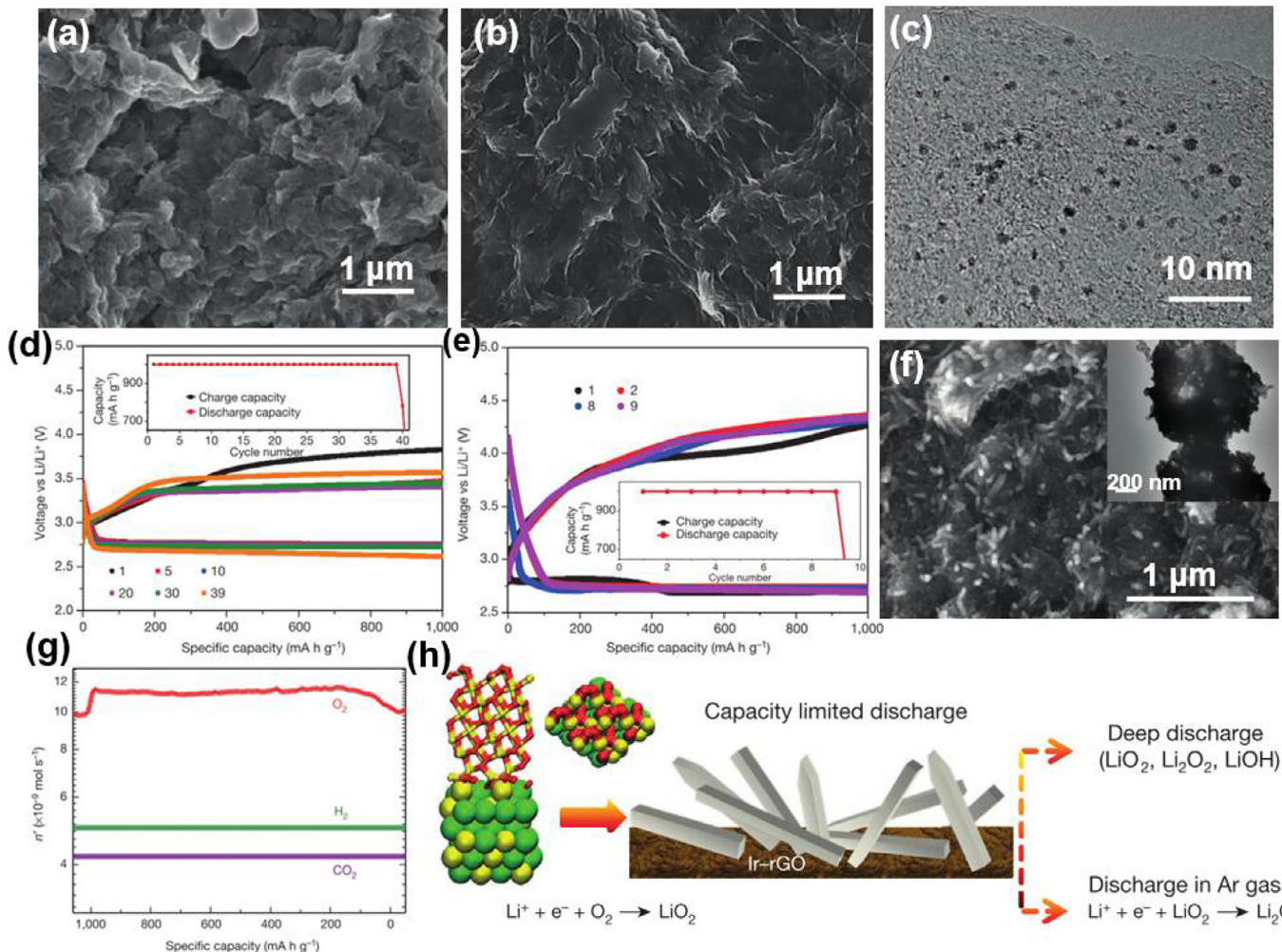


Fig. 5. SEM images of (a) rGO, and (b) Ir-rGO composite. (c) TEM image of Ir-rGO composite. Voltage plots of (d) Ir-rGO and (e) rGO. Inset exhibits cycling performance. (f) SEM and TEM images of discharge products on Ir-rGO. (g) Differential electrochemical mass spectroscopy (DEMS) plots exhibiting different gases released from the battery during charging under 1000 mA g⁻¹ after initial discharge. (h) Schematic exhibiting lattice match between Ir₃Li and LiO₂. Reproduced with permission from Ref. [33], Copyright 2016, Nature Publishing Group.

of 507 mV dec⁻¹ (Fig. 6h-j). In addition, Wu et al. reported monodispersed Mn₃O₄ nanoparticles supported on rGO by a one-step synthesis approach [120], and significantly, the resulting Li-O₂ cells based on this catalyst displayed first cycle discharge capacity of 16,000 mAh g⁻¹, which was larger than those of commercial Pt/C electrocatalysts (2000 mAh g⁻¹).

More reasonably, graphene is an excellent building block for the facile assembly of 3D architectures as the cathodic electrode and/or flexible supports for electrocatalysts. For instance, Kim et al. reported a 3D graphene hollow sphere as Li-O₂ batteries cathode [121], in which this rational O₂ cathode displayed a large initial discharge capacity of 18,578 mAh g_{carbon}⁻¹ for Li-O₂ cells because the unique spherical morphology and the graphene with fewer defects and impurities synergistically provided a large void space for discharge products and enabled the fluent transportation of electrons, Li⁺ and O₂ species. Further, Yan et al. synthesized graphene foams through electrochemical leavening of graphite papers, and then annealed under inert atmosphere [122]. As a result, this graphene foam with lower amount of structural defects serving as binder-free O₂ cathode displayed a round-trip efficiency up to 80% and a steady discharge/charge potential at ~ 2.8/3.8 V for 20 cycles. Similarly, Zhu et al. constructed a 3D graphene foam on aluminum foam as a binder-free cathode with large surface area to accommodate a mass of discharge products [123]. Thus, this resultant cath-

ode performed a record capacity of ~ 9 × 10⁴ mAh g_{graphene}⁻¹ at 1st discharge under 100 mA g_{graphene}⁻¹. To avoid the interference of H₂O, Duan et al. fabricated a 3D hydrophobic graphene as a water-repellent cathode to improve performance Li-O₂ cells (Fig. 7), thus delivering a lifetime capacity of (1~3) × 10⁵ mAh g⁻¹ [124]. Moreover, gray et al. employed the hierarchically macroporous rGO cathode to enhance the efficiency and capacity for Li-O₂ cells [38]. Importantly, the key roles of rGO framework were highlighted from two aspects. On one hand, 3D rGO framework could supply efficient diffusion pathways for all active species, resulting in a lower cell overpotential and excellent electrochemical profile. On the other hand, 3D rGO framework could greatly promote the growth of discharge products in larger size, leading to high capacity that is much closer to the theoretical value of Li-O₂ cells. Therefore, it is anticipated that 3D architectural graphene shows enormous potential as the cathodic materials for Li-O₂ batteries.

To further enhance the performance of nonaqueous Li-O₂ cells, 3D architectural graphene has been modified with doped heteroatom and hybridized with oxygen catalyst materials. For example, Qiu et al. prepared a porous N-doped graphene aerogels via hydrothermal self-assembly approach to construct the interconnected nanocages [125], and found this 3D porous graphene aerogels delivered high specific capacity, outstanding rate capacity of 5978 mAh g⁻¹ under 3200 mA g⁻¹, and good cycling stability (54 cycles) under 1000 mA g⁻¹. Similarly,

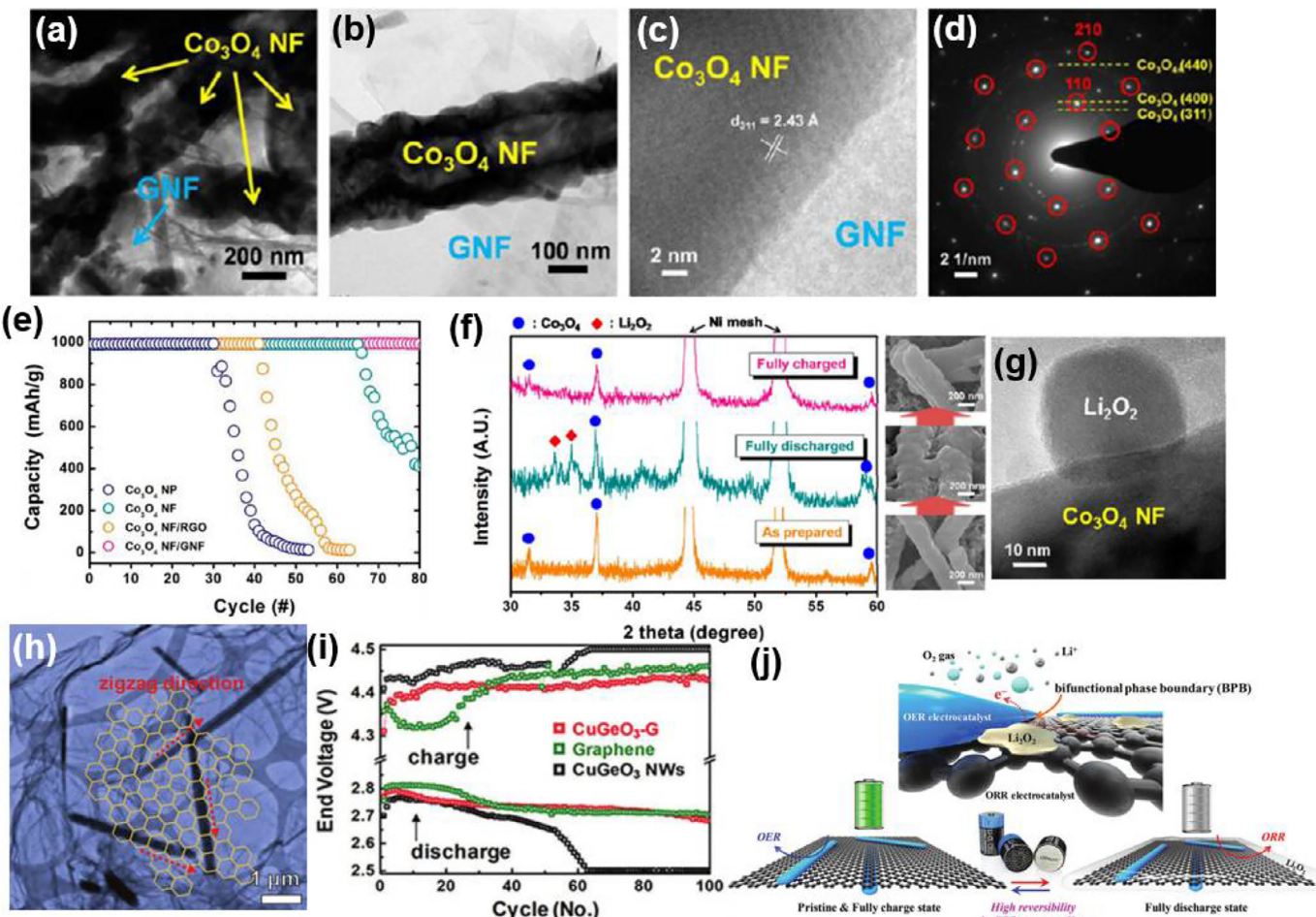


Fig. 6. (a,b) TEM images, (c) lattice fringe and (d) SAED plots of Co₃O₄-based hybrids. (e) Cycling stability of Co₃O₄ nanoparticles and other composite under 1000 mAh g⁻¹ and 200 mA g⁻¹ between 4.35 and 2.0 V. (f) Exsitu X-ray diffraction (XRD) patterns and SEM images of Co₃O₄ NF/GNF cathodes. (g) TEM image of Li₂O₂ formed on the Co₃O₄ NF. Reproduced with permission from Ref. [118] Copyright 2013, American Chemical Society. (h) TEM image of nanowire-axis directions of CuGeO₃ nanowires (NWs) on graphene. (i) Galvanostatic cycling stability of Li-O₂ batteries based on CuGeO₃ NWs, graphene, and CuGeO₃-G cathodes. (j) Possible mechanism of enhanced ORR and OER process of CuGeO₃-G. Reproduced with permission from Ref. [119] Copyright 2018, Wiley-VCH.

Lu et al. prepared 3D B-doped rGO (B-rGO) with hierarchically porous, ultrathin structure employed as cathode material [126], and using DFT calculation revealed B-rGO could more efficaciously resolve Li₂O₂ by activating Li-O bonds during charge compared to undoped rGO due to stronger interactions between B-rGO and Li₅O₆ clusters. Besides, N and S co-doped 3D bicontinuous porous graphene (N,S-3DG) with high electrical conductivity and specific surface area reported by Chen et al. was as cathode for nonaqueous Li-O₂ batteries, exhibiting large capacity of 10,400 mAh g⁻¹ and long cycling stability of 300 cycles at 1000 mAh g⁻¹ [127]. Further, they also developed a 3D nanoporous cathode through embedding RuO₂ nanoparticles into N-doped graphene [128]. Notably, this freestanding 3D graphene/RuO₂ used as cathode of Li-O₂ cells exhibited highly reversible discharge/charge of 100 cycles at 2000 mAh g_{total}⁻¹ and small charge voltage of 3.7 V. To accommodate more insoluble and insulating discharge products for increasing the capacity of Li-O₂ batteries, Yan et al. developed 3D graphene-encapsulated carbon foam (GF) derived from 3D melamine foam as the backbone for stably supporting the core-shell Co/CoO nanoparticles [129]. Expectedly, the as-made 3D GF-Co/CoO cathode achieved large capacity (7800 mAh g_{total}⁻¹) and excellent rate capability, as proved by high capacity retention of 55.3% at 200 mA g⁻¹ based on the capacity at 50 mA g⁻¹. Additionally, Fellinger et al. assembled a novel configuration of cathode comprised of transition metal hydroxide and vertically aligned graphene hybrid arrays, which integrated the excellent ORR with OER

active phases employed as bifunctional electrocatalysts for Li-O₂ cells. Impressively, this cathode offered long-term cyclability, small discharge potentials of 0.19 V, and large capacity of 12,123 mAh g⁻¹ based on the mass of metal hydroxide [130]. Overall, graphene-based cathode materials can serve as the promising materials in Li-O₂ cells cathode. In order to realize practical application, it is urgent to explore low-cost and scalable high-quality graphene materials and design new 3D graphene assemblies for Li-O₂ batteries. Beyond this, developing other 2D materials with comparable performance is also a highly intriguing solution.

3.1.2. 2D transition metal oxides/hydroxides

To facilitate the decomposition and formation of discharge products in cathode, TMOs/TMHs have been broadly explored for monofunctional or bifunctional ORR/OER electrocatalysts for boosting Li-O₂ batteries [56,131], owing to their efficiently catalytic activity, controllable structure, low cost, and multiple valences [60,120,132]. In particular, 2D oxides/hydroxides can provide large surface area which are benefiting for ion transport and physical contact, expose large amount of atomic steps and kink atoms, thus providing a broad platform to break chemical bonds and improving activity for electrocatalytic reaction in Li-O₂ batteries [133,134].

Up to now, manganese oxides are most widely studied as cathodic catalysts for Li-O₂ cells, because they could efficiently increase the specific capacity, and enhance the round-trip efficiency [135–137]. To

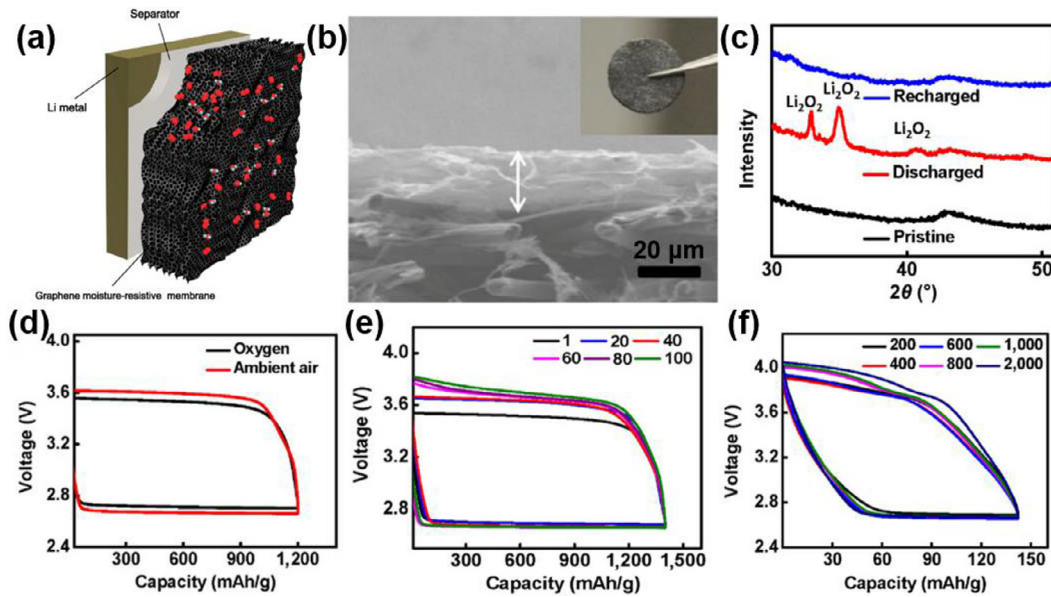


Fig. 7. (a) Schematic of a Li-O₂ cell with 3D graphene electrode. (b) Photograph and cross-section SEM image of 3D graphene membrane. (c) XRD patterns of pristine, discharged and recharged graphene-based cathodes. (d) Galvanostatic discharge and charge profiles of graphene membrane cathode-based Li-air cell in O₂ and air. (e,f) Galvanostatic cycling of a Li-O₂ cell at (e) 1425 mAh g⁻¹ and (f) 140 mAh g⁻¹. Reproduced with permission from Ref. [124] Copyright 2016, Tsinghua University Press and Springer.

avoid the interlayer re-stacking between 2D sheets of manganese oxide that greatly lowers the performance, Qiao et al. assembled 2D δ-MnO₂ nanosheets into 3D aerogels that sufficiently inhibited the aggregation of 2D ultrathin structure [138]. As a consequence, 3D MnO₂ aerogels delivered larger discharge capacity of 4581 mAh g⁻¹ for Li-O₂ battery than its powder-like counterpart (3902 mAh g⁻¹). Meanwhile, the as-fabricated Li-O₂ cell demonstrated outstanding rate capability and cycling life of 25 cycles at a 1000 mAh g⁻¹ due to the abundant porosity and 3D continuous mesh of the 3D MnO₂ aerogel, which made full use of active sites, thus increased the capacities. However, the electrical conductivity of MnO₂ is limited by the nature of oxides. To improve its conductivity, Hwang et al. prepared multilayer hybrid nanosheets with mesoporous conductive carbon and layered δ-MnO₂ (L-MnO₂) as cathode of Li-O₂ batteries [139], which delivered low overpotential, improved cyclability and huge discharge capacity of ~ 7000 mAh g⁻¹ at 200 mA g⁻¹. Besides the combination with carbon-based materials, regulating the valence of oxides is another strategy to increase electrical conductivity, compared to the normally stoichiometric MnO₂. For instance, 2D low-valent Mn₂O₃ nanosheets, synthesized through thermally induced phase transition of stripped 2D MnO₂, could offer holey structure, large amount of electron depletion centers (Mn³⁺) and more active sites [140], and thus delivered obviously decreased overpotential of OER in Li-O₂ batteries. Additionally, Zhao et al. designed a unique IrO₂-decorated 2D δ-MnO₂ (IrO₂/MnO₂) as electrocatalyst in Li-O₂ battery (Fig. 8), and delivered high capacity of 16,370 mAh g⁻¹ and a wide-window cycling stability of 312 cycles at 1600 mA g⁻¹ [144]. Because of high cost of Ir, the non-precious CeO₂ nanoparticles with ultrafine size were decorated on graphene-like δ-MnO₂ nanosheets [141]. Although the performance of Li-O₂ cell was inferior to IrO₂/MnO₂, this novel CeO₂/δ-MnO₂ catalyst still displayed a discharge specific capacity of 8260 mAh g⁻¹ at 100 mA g⁻¹ and comparable cycling life of 296 cycles at 500 mAh g⁻¹.

The oxides as electrocatalyst are inevitably subjected to low surface areas and poor conductivity, which is usually settled by coupled with conductive support. For instance, Qin et al. synthesized ultrathin Co₃O₄ nanosheets highly dispersed grown on rGO as the electrocatalyst for Li-O₂ battery [142], exhibiting high initial capacity of 10,528 mAh g⁻¹ because of the synergistic effect between rGO and Co₃O₄. Otherwise, Li et al. compared flowerlike, cuboidlike and ordered 2D

porous nanosheets Co₃O₄ for Li-O₂ cathodes [143]. It is revealed that the 2D counterpart with ordered structure showed better cycling stability for more than 50 cycles at 1000 mAh g⁻¹ and higher discharge capacity of 10,417 mAh g⁻¹ at 200 mA g⁻¹. Similarly, Liu et al. designed 2D ultrathin Co₃O₄ nanosheets as electrocatalyst of Li-O₂ cells [133]. Interestingly, 2D catalyst showed high activity with a low discharge overpotential of 0.36 V in the initial discharge process because the edge-enriched {111} facets with more exposed metal atoms, atomic steps and kink atoms were beneficial for breaking chemical bonds. Moreover, 2D orthorhombic MoO₃ nanosheets with abundant oxygen vacancies (MoO_{3-x}NS) displayed low overpotential of 0.5 V due to catalytic decomposition of Li₂O₂ on the oxygen vacancy sites [144]. Based on the conductive 2D oxides, spinel oxides, in particular MnCo₂O₄ have been reported as composited part as efficient electrocatalysts for Li-O₂ cells because of the variable valence states of Mn and Co, for example, MnCo₂O₄ nanoparticles supported on porous MoO₂ nanosheet with substoichiometric oxide layer as a cathode catalyst exhibited outstanding cyclability of > 400 cycles and low potential gap of 0.75 V at 5000 mA g⁻¹ [145]. It is worth noting that, electrical RuO₂ is a metallic oxide with outstanding conductivity of 10⁴ S cm⁻¹. Based on this, Zhou et al. synthesized 2D conducting rutile RuO₂ nanosheets for Li-O₂ batteries, which delivered a low discharge/charge overpotential of 0.15/0.59 V up to 50 cycles [146]. Further, Kim et al. reported the 2D RuO₂ catalyst with remarkable electrical conductivity of ~35 S cm⁻¹ assembled with carbon nanotube in Li-O₂ battery [147].

Besides metal oxides, layered double hydroxides (LDH), widely employed in aqueous Zn-air batteries [148–151], could also efficiently improve the catalysis activity in nonaqueous Li-O₂ cells. As an example, Chitravathi et al. demonstrated that NiFe-LDH with 3R structure offered discharge capacity of 3218 mAh g⁻¹ at current density of 0.1 mA cm⁻² and overpotential gap of 0.9 V [152]. As another example, Chen et al. further decreased the overpotential gap to 0.45 V with hierarchically porous CoTi-LDH with hexagonal structure as electrocatalysts, which exhibited superior cycling stability of 80 cycles at 100 mA g⁻¹ [153]. Despite the excellent performance of carbon-based materials in cathode, the active oxygen species, such as superoxide, readily attack the carbon-based materials, giving rise to by-products, such as Li₂CO₃. In order to avoid this kind of side reaction, Ma et al. fabricated a carbon-free

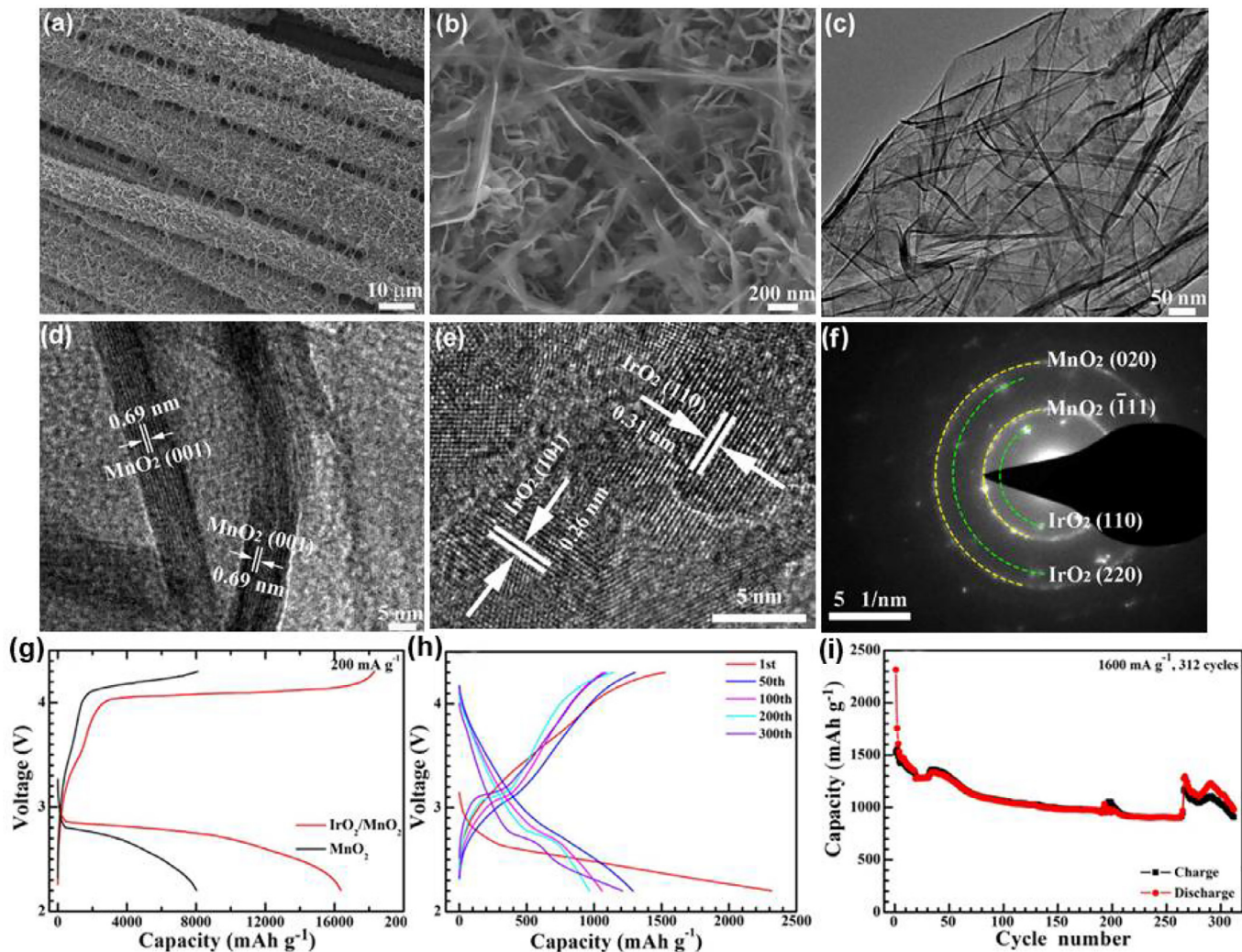


Fig. 8. (a,b) SEM, (c) TEM, (d,e) HRTEM images and (f) SAED patterns of $\text{IrO}_2/\text{MnO}_2$ catalysts. (g) Voltage curves of $\text{Li}-\text{O}_2$ batteries employed $\text{IrO}_2/\text{MnO}_2$ as electrocatalyst obtained at 200 mA g^{-1} . (h) Voltage plots and (d) cycle stability of $\text{Li}-\text{O}_2$ batteries based on $\text{IrO}_2/\text{MnO}_2$ electrocatalyst at 1600 mA g^{-1} . Reproduced with permission from Ref. [134], Copyright 2017, Elsevier.

cathode by casting 2D superlattice structured $\text{CoNiFe-LDH/RuO}_{2,1}$ on stainless steel mesh, which could steadily run more than 50 cycles without obvious degradation, while the LDH/rGO cathode degraded rapidly after only 31 cycles [154].

3.1.3. Transition metal chalcogenides

Recently, 2D TMCs nanosheets have been applied in nonaqueous $\text{Li}-\text{O}_2$ cells system owing to their prominent catalytical activity features and higher conductivity than oxides. For instance, Salehi-Khojin et al. constructed a nonaqueous $\text{Li}-\text{O}_2$ battery based on MoS_2 nanoflakes and ionic liquid [155]. Notably, this defect-free 2D structural catalyst exhibited excellent OER and ORR performance, e.g., high round-trip efficiency up to 85% and excellent reversibility of 50 cycles, superior to Au and Pt catalysts (Fig. 9). Likewise, to accelerate the sluggish ORR and OER, 2D trigonal phase MoS_2 nanosheets (1T- MoS_2 NS) were developed as high-activity electrocatalyst in $\text{Li}-\text{O}_2$ batteries [156]. Because of the catalytically active surfaces, this 2D nanosheet catalyst disclosed large reversible capacity of 500 mAh g^{-1} at 200 mA g^{-1} and good term stability of more than 100 cycles, demonstrative of fast accessibility to O_2 and Li^+ ions. To further enhance the performance of 2D TMCs for $\text{Li}-\text{O}_2$ cells, 2D mesoporous $\text{MnCo}_{2}\text{S}_4$ nanosheets ($\text{MnCo}_{2}\text{S}_4$ NS) were explored as a more efficient catalyst [157], delivering considerably large first discharge capacity of $10,760 \text{ mAh g}^{-1}$ and enhanced stability of 96 cycles

under limited capacity of 500 mAh g^{-1} at 200 mA g^{-1} due to higher electrical conductivity and ionic diffusion coefficient. Additionally, Li et al. analyzed the possibility and fundamental mechanism of monolayer 2D TMCs (GeS , GeSe) as electrocatalysts in nonaqueous $\text{Li}-\text{O}_2$ cells [158]. It is demonstrated that 2D GeSe nanosheet was more active than 2D GeS owing to its greatly lower overpotential of OER (1.30 V) and ORR (0.94 V) from the point of binding capacity between catalysts and Li_xO_y intermediates in $\text{Li}-\text{O}_2$ batteries.

3.1.4. Other 2D materials

Considering the structural advantages of 2D materials for catalytic reactions, various other 2D materials composed with different elements and phases were also explored as electrocatalyst for $\text{Li}-\text{O}_2$ cells from the perspective of experiment and theory calculation, such as graphitic- C_3N_4 , 2D metal organic frameworks (MOFs), MXene, and elemental analogues of graphene. In one word, the main purpose is to replace the noble metal-based materials.

For instance, Zhou et al. fabricated a high C (sp^2)-hybridized graphitic- C_3N_4 supported on carbon papers with greatly improved electrocatalytic activity of ORR/OER as cathodes of $\text{Li}-\text{O}_2$ cells [159]. Owing to the good conductivity and high nitrogen content, the as-assembled $\text{Li}-\text{O}_2$ cells showed outstanding rate capability and durable cycling stability up to 100 cycles. Recently, 2D MOFs have been regarded as promising

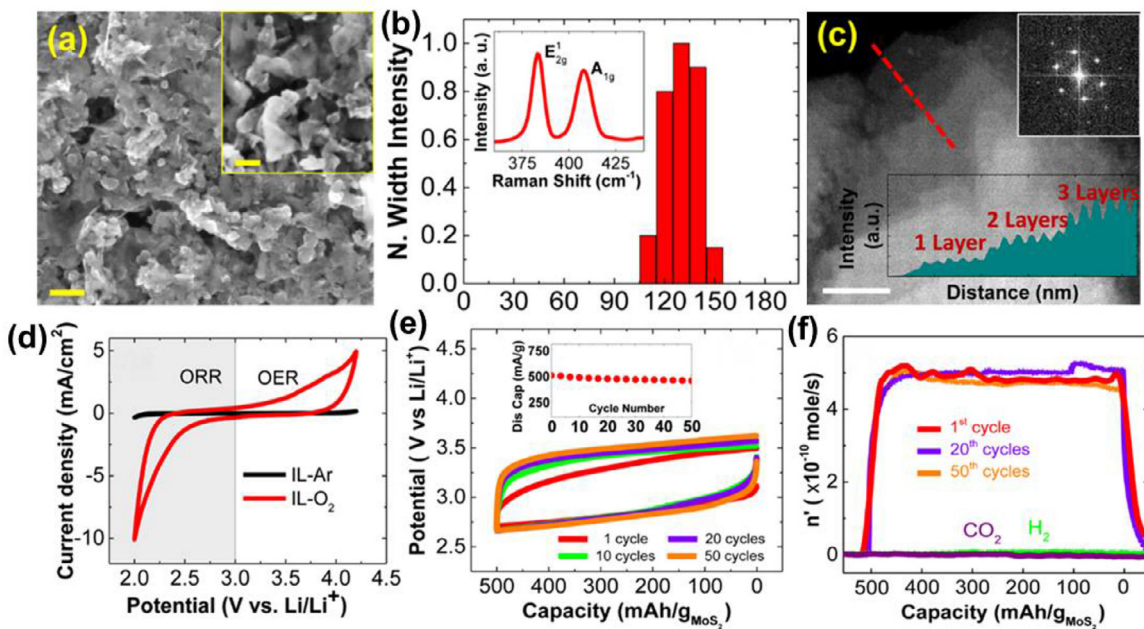


Fig. 9. (a) SEM images of MoS_2 nanosheets. (b) Dynamic light scattering and Raman pattern of MoS_2 nanosheets. (c) STEM image of a MoS_2 nanosheet, insets are line plots and FFT pattern, scale bar is 100 nm in (a) and 50 nm in (c). (d) CV curves achieved in ionic liquid (IL) at 20 mV s^{-1} . (e) Charging/discharging voltage plots based on MoS_2 nanosheets cathode. (f) DEMS curves of the battery after different cycle. Reproduced with permission from Ref. [155], Copyright 2016, American Chemical Society.

platforms for electrocatalysis [160–162], because 2D MOFs can inherit all the merits of bulk counterpart, meanwhile, expose more active sites [163–166]. Typically, Ma et al. prepared ultrathin Co, Ni, Mn-based 2D MOFs, and tested their performance as the cathodic catalysts in Li-O_2 cells [167]. Remarkably, it was revealed that 2D Mn-based MOFs cathode delivered higher discharge capacity of 9464 mAh g^{-1} and longer cycling life (> 200 cycles) at 100 mA g^{-1} and 1000 mAh g^{-1} originating from the intrinsic active sites in 2D Mn-O framework (Fig. 10a–c).

It is well accepted that first-principles calculations offer a fundamental comprehension for various catalytic reactions and mechanism. More significantly, it can effectively guide the researchers to accurately screen and choose appropriate materials for targeted application [168–170]. Using this approach, 2D materials can be efficiently selected as cathodic materials for Li-O_2 cells. For instance, Li et al. examined the oxygen reaction mechanism of single layer graphitic germanium carbide (g-GeC) in Li-O_2 battery via calculation of the adsorption and dissociation energy of oxygen on g-GeC [171]. It is demonstrated that from the calculation the g-GeC delivered very low overpotentials for discharge (0.89 V) and charge (0.21 V), owing to charge redistribution resulting from electronegativity difference. Differently, Viswanathan et al. conducted a computational study to assess the thermodynamic overpotential of various MXene nitrides for selective Li_2O_2 nucleation [172]. Importantly, it is found that the highly terminated $\text{Ni}_4\text{N}_3(\text{OH})_2$ was the most promising candidate due to least nucleation overpotential of 0.18 eV. In addition, Chung et al. proposed 2D h-BN/Ni(111) electrocatalyst for Li-O_2 cell and revealed the adsorption energy of ORR intermediates on the catalyst [173]. Because the B atoms in h-BN was coupled to the O atoms of the intermediates by strong ionic bonds, 2D h-BN/Ni(111) exhibited the highest discharge potential (1.93 V) and lowest charge potential (3.83 V) (Fig. 10d). Besides, this group also calculated the reaction mechanism of silicene for Li-O_2 battery [174], and considered that ORR and OER possibly occurred on the pure silicene with no defect sites, which was opposite to graphene-based materials. Fortunately, Wang et al. synthesized ultrathin silicene-shaped nanosheets and explored their performance of Li-O_2 batteries (Fig. 10e–i). Impressively, this silicone-like nanosheets of allo-Si metastable phase displayed outstanding performance in nonaqueous Li-O_2 battery with high energy efficiency of 73% and stability up to

20 cycles [175]. Moreover, Singh et al. proposed the 2D phosphorene as electrocatalyst for Li-O_2 battery and achieved free-energy diagrams of different mechanism [176], in which predicted the discharge overpotentials (1.44 V) and charge overpotentials (2.63 V). More importantly, the DFT results displayed activated energy barrier of 1.01 eV to electrocatalytic decompose the discharge products with 2D phosphorene due to its easy-diffusion structure for Li^+ , which was smaller than graphene counterpart (2.06 eV).

In short, 2D materials with easily assembled property and high electrical conductivity provide hierarchical structure and multiple pathway for the diffusion of electrolyte, O_2 , electrons and accommodation space for discharge products. Furthermore, various 2D materials composed by different elements and phases with outstanding catalytic activities for OER and ORR efficiently reduce the polarization and improve the round-trip efficiency for Li-O_2 cells (Table 1). More importantly, 2D materials with 2D unique configuration supply an ideal platform to explore the fundamental mechanism of electrochemical reactions for Li-O_2 batteries via first principles calculation.

3.2. 2D materials for electrolyte additive & separator

As mentioned above, the quasi/all-solid-state electrolytes have shown great advantages on overcoming various issues of organic electrolyte, e.g., easy decomposition, volatilization, frequency side reaction with Li anode, oxygen, intermediate species and Li dendrites. While the separator between the cathode and anode plays a key role on protecting Li-O_2 batteries from short circuits. Therefore, the design of solid-state electrolytes and separators have an enormous effect on the performance of Li-O_2 batteries. In general, the solid-state electrolyte and separator are located between the cathode and the anode. Thus, the materials employed in solid-state electrolytes and separators for nonaqueous Li-O_2 batteries have some common functions. Both of them are used to prevent the electron, oxygen, reactive oxygen species and other intermediate reactant from permeating between cathode and anode, promote the Li^+ ion fluxes, especially suppress the Li dendrites and provide the flexibility [74–76,82,83,177,178]. In this case, certain 2D materials applied in solid-state electrolytes and separator should furnish with simi-

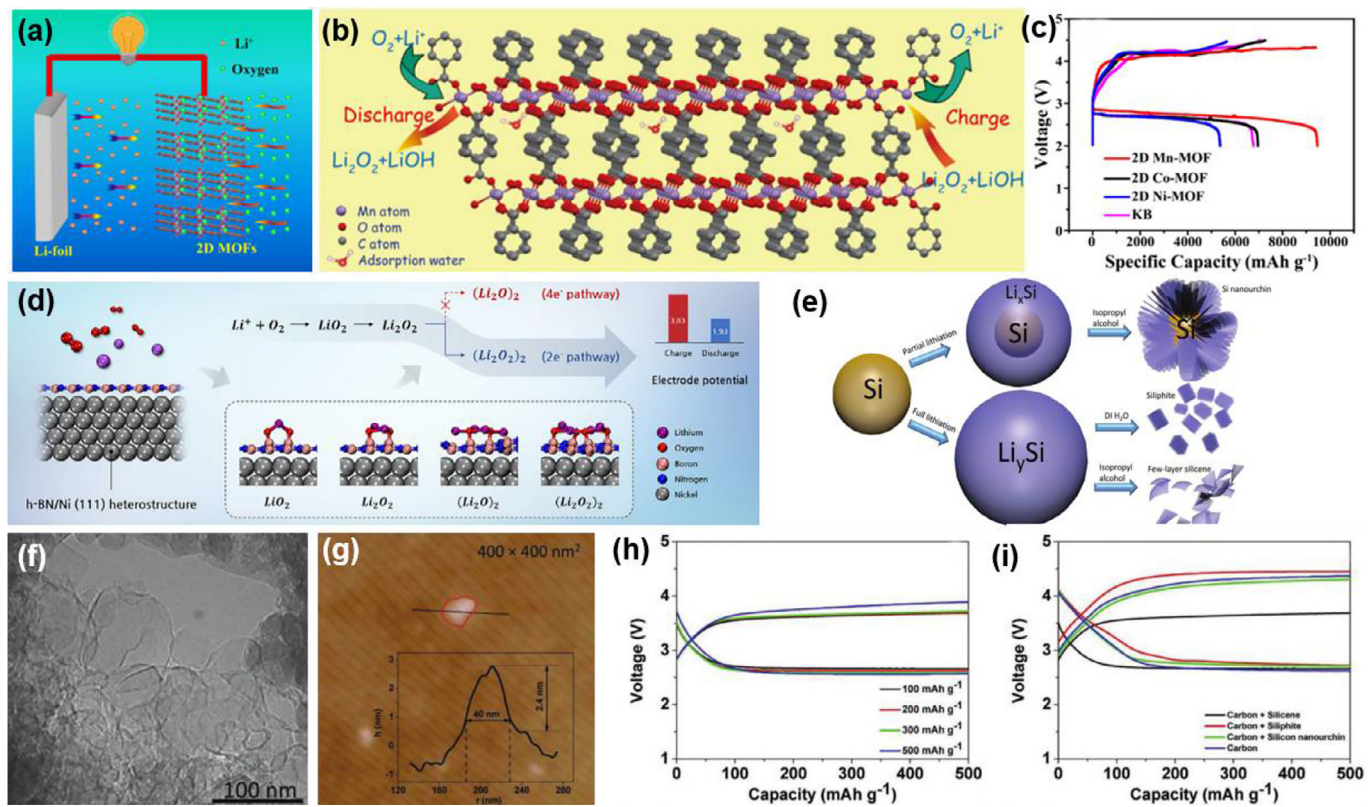


Fig. 10. Schematic of (a) Li-O₂ cell and (b) proposed electrochemical process applied 2D MOF as catalysts. (c) Discharge-charge plots with 2D MOFs and Ketjen Black catalysts at 100 mA g⁻¹. Reproduced with permission from Ref. [167], Copyright 2019, American Chemical Society. (d) Scheme of h-BN/Ni(111) as electrocatalyst of nonaqueous Li-O₂ battery. Reproduced with permission from Ref. [173], Copyright 2016, Elsevier. (e) Scheme of preparation of silicon. (f) TEM and (c) AFM images of ultrathin silicene. (h) Voltage profiles tested at 100 mA g⁻¹, and (i) voltage plots of silicene catalyst for Li-O₂ cells measured at different current densities. Reproduced with permission from Ref. [175], Copyright 2018, Wiley-VCH.

Table 1

The performance of nonaqueous Li-O₂ batteries with 2D materials in cathode.

Cathode materials	Electrolytes Li salts/solvents	Capacity (mAh g ⁻¹)/current density (mA g ⁻¹)	Cycling life			Ref.
			Current density (mA g ⁻¹)	Restricted capacity (mAh g ⁻¹)	Cycle number	
CuGeO ₃ -G	1 M LiNO ₃ /DMAc	10,030/200	200	1000	100	[119]
B-rGO	1 M LiTFSI/TEGDME	~ 18,000/100	–	–	–	[126]
N,S	1 M	10,400/-	2000	1000	300	[127]
3DG	LiTFSI/TEGDME		300	2000	100	
IrO ₂ /MnO ₂	1 M LiClO ₄ /TEGDME	16,370/200	1600	2.0 ~ 4.4V	312	[134]
L-MnO ₂	1 M LiCF ₃ SO ₃ /TEGDME	~ 7000/200	200	1000	~ 27	[139]
MoO _{3-x} NS	1 M LiClO ₄ /DMSO	9000 ~ 11,000/100	100	1000	80	[144]
NiFe-LDH	1 M LiPF ₆ /TEGDME	~ 3218/0.1 mA cm ⁻²	0.1 mA cm ⁻²	~ 1728	30	[152]
1T-MoS ₂ NS	0.5 M LiTFSI/TEGDME	–	200	500	~ 100	[156]
MnCo ₂ S ₄ NS	0.5 M LiTFSI/TEGDME	10,760/200	200	500	96	[157]
2D Mn-MOF	1 M LiTFSI/TEGDME	~ 9500/200	100	1000	~ 200	[166]
Silicene	1 M LiTFSI/TEGDME	–	200	100	20	[175]

Note: DMAc (Dimethylacetamide), LiTFSI (Lithium bis-trifluoromethanesulfonimide), TEGDME (Tetraethylene glycol dimethyl ether), DMSO (Dimethyl sulfoxide).

lar properties, including electrical insulativity, high ionic conductivity, outstanding mechanical and chemical stability.

Recently, a rapidly increasing trend of using solid electrolytes in rechargeable batteries has emerged to stabilize the electrolytes, suppress the side reaction and protect the Li anode [69]. However, solid-state electrolytes are always limited by low ionic conductivity and limited Li⁺ flux for Li metal batteries [63]. Especially, the complicated operation condition of Li-O₂ batteries puts forward high requirements for solid-state electrolytes, such as higher stability when exposed to moisture, better thermal stability, wider electrochemical window and temperature operating range (-40 ~ 60 °C). In addition, commercial separators

employed in nonaqueous Li-O₂ batteries still possess poor mechanical properties, wettability and thermal integrity [179]. In this context, 2D materials have been proposed to efficiently address the main issues because of their high specific surface area, superionic conduction, tunable wettability, excellent stability and flexibility [80,180]. For instance, Kumar et al. developed an excellent Li-ion conductive laminate film prepared from polymer-ceramic (PC) and glass-ceramic (GC) materials as solid-state electrolyte. The key PC membranes in solid-state electrolyte were made of poly ethylene oxide (PEO), LiN (SO₂CF₂CF₃)₂ (LiBETI), boron nitride (BN) and Li₂O (Fig. 11a, b). Using this electrolyte, the cell exhibited superior rechargeability and thermal stability from 30 to

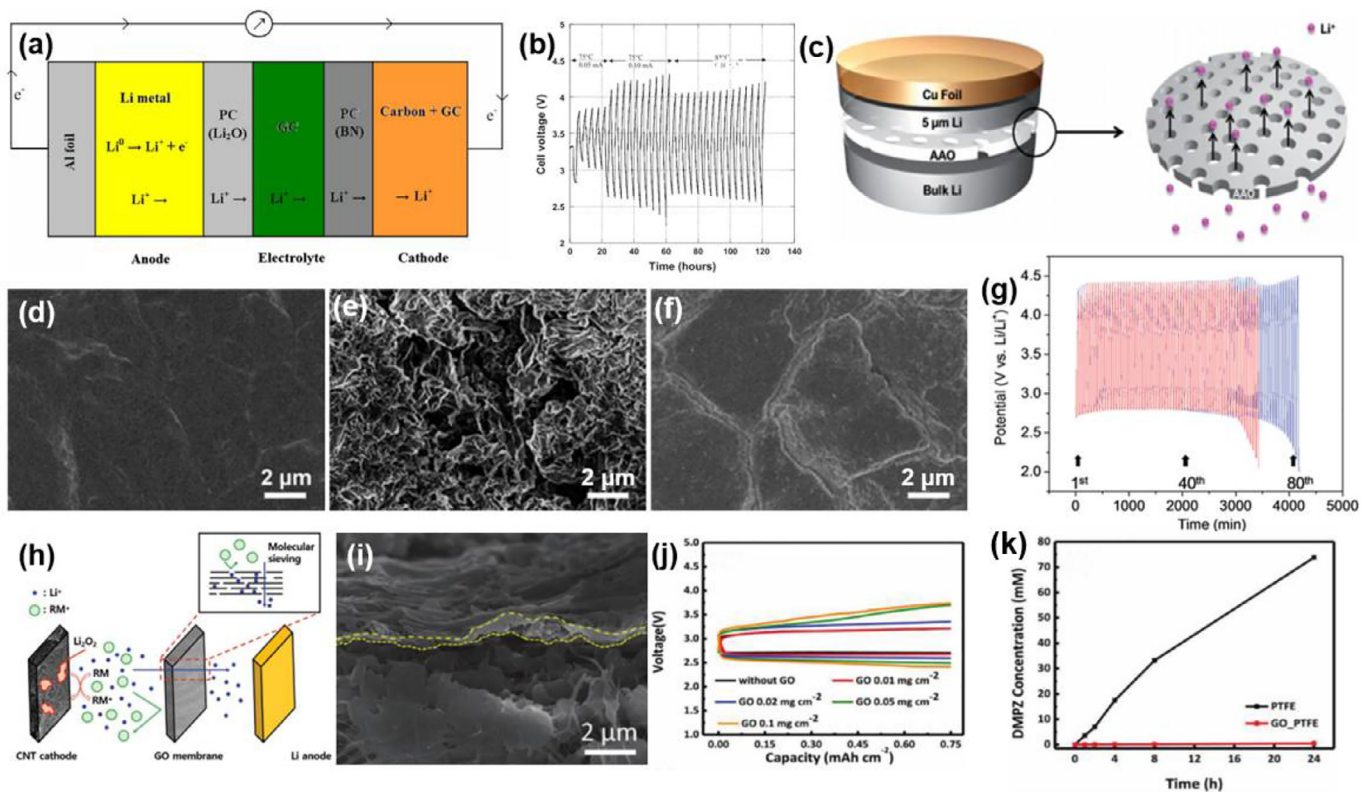


Fig. 11. (a) Schematic of Li-O₂ cell based on BN additive. (b) Rechargeable performance of Li-O₂ cell via testing the relationship between discharge/charge current and temperature. Reproduced with permission from Ref. [77], Copyright 2010, The Electrochemical Society. (c) Schematic of coin cell employed AAO as separator. SEM images of surface of Li on Cu foil: (d) pristine Li, (e) PS and (f) AAO separator employed 10 cycles later. (g) The cycling performance of Li-O₂ batteries employed with (blue) and without (red) the AAO separator. Reproduced with permission from Ref. [183], Copyright 2014, The Royal Society of Chemistry. (h) Schematic of charge process in RM-mediated Li-O₂ battery with a GO membrane. (i) SEM image of a GO-PTFE composite film. (j) The initial voltage plots of GO-PTFE film with different amounts of GO. (k) Change of dimethylphenazine (DMPZ, a kind of RM) after 24 h diffusion through PTFE and GO-PTFE films. Reproduced with permission from Ref. [184], Copyright 2018, Wiley-VCH.

105 °C [77]. It is noted that BN nanosheets with highly chemical resistance, high-temperature thermal stability and low expansion coefficient played a key role in the performance improvement of PC membranes. Based on this concept, this group sequentially employed BN as the modifier in solid-state electrolyte for Li-O₂ cells [181]. It is found that the cycling stability of Li-O₂ batteries was significantly enhanced owing to the BN additive into PEO: LiBETI polymer matrix. Therefore, it is disclosed that BN can effectively enhance interface-mediated lithium ion transfer and the performance of Li-O₂ cells. Besides the role of ionic-conduction, 2D materials added into electrolytes can efficiently inhibit the lithium dendrites during plating. For example, Shu et al. added 2D Ti₃C₂T_x MXene into a gel polymer electrolyte to guide the uniform nucleation and growth of Li metal. As a result, the Li-O₂ battery could run over 200 cycles with stable overpotential of 0.95 V at room temperature [182].

Other than acting as the additive of electrolyte, 2D materials also can serve as coatings on separators to promote the performance of Li-O₂ batteries. As a typical instance, Kim et al. adopted anodized porous alumina (AAO) as a 2D separator with ordered nanopores [183]. As expected, 2D AAO membranes as the separator of Li-O₂ batteries provided suitable channels of Li⁺ ion transfer, thus resulting in uniform plating/stripping of Li. The surface of Li displayed smoother with AAO separator than that with polymeric separators (PS) after 10 cycles, therefore, 2D AAO separator efficiently enhanced the cycle life of Li anode (Fig. 11c-g). To decrease the energy barrier for the formation and decomposition of Li₂O₂ and keep the stability at the same time, Lee et al. developed the GO membranes as separators to block redox media (RM) [184]. It is proved that the ultra-thin GO films successfully inhibited the diffusion of RM to Li metal and significantly improved the vitality of high-efficiency Li-

O₂ batteries (Fig. 11h-k). Another way to reduce the overpotential of charge is to improve the conduction of insulating discharge products. As reported by Chen et al., a conductive graphene interlayer was built up between the separator and the cathode to closely contact and easily decompose the Li₂O₂, therefore, this Li-O₂ battery exhibited long life of 200 cycles and low overpotential of 0.67 V at a current density of 500 mA g⁻¹ [185].

It is highlighted that 2D materials are usually used in the electrolyte additives and separator coatings, in particular, the interface between electrode and electrolyte interfaces, which can efficiently promote the synergy of Li⁺ diffusion and reduce the charge buildup on Li anode. Through assisting in the homogeneous dispersion of Li ionic flux in the structure, they are also able to promote cation transfer and reduce reaction delays. Additionally, the outstanding mechanical performance of 2D materials could effectively prevent the nucleation and growth of dendrites [186]. Despite the studies on 2D materials for electrolyte additives and separator coating are meager so far, the merits of 2D materials on high electrical/ionic conductivity and protection for Li anode will drive the researchers pay more attention on this topic.

3.3. 2D materials for anode protection

Metallic Li has been considered as the most ideal anode owing to its lowest reduction potential (-3.04 V vs. SHE) and the highest capacity in theory (3860 mAh g⁻¹). Nevertheless, the commercialization of Li metal batteries, such as Li-O₂ batteries, is intrinsically limited by its poor safety and stability [187,188]. To overcome this issue, numerous strategies were developed for the protection of Li metal anodes [95,189,190]. Unfortunately, these strategies for the common Li metal batteries, e.g.,

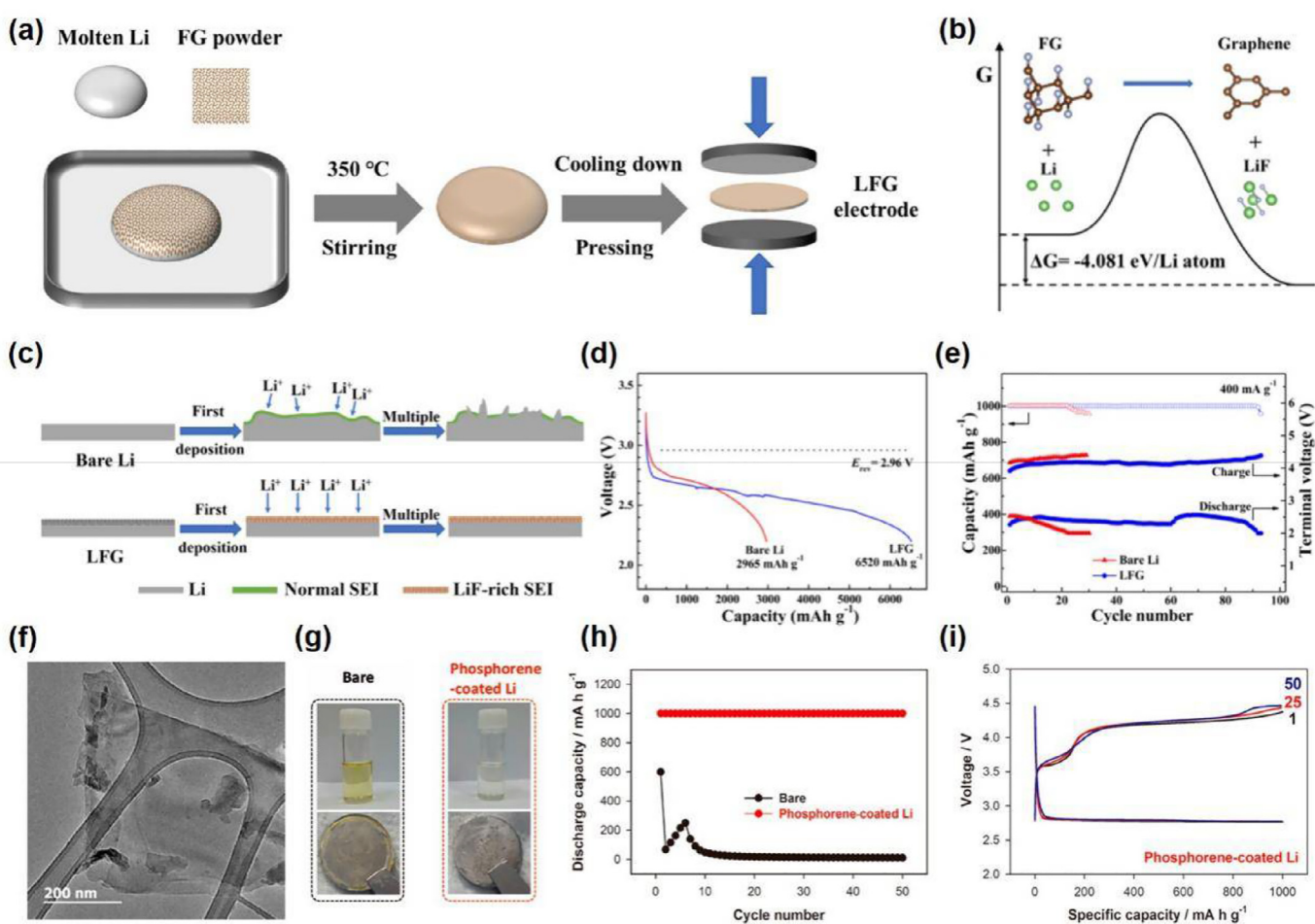


Fig. 12. (a) Schematic of LFG anode fabrication. (b) DFT calculation of main chemical reaction. (c) Schematic of cycling stability of LFG compared to bare Li anodes. (d) Discharge curves of Li-O₂ batteries with different anodes obtained at 100 mA g⁻¹. (e) Cycling performance of Li-O₂ cells with the bare Li and LFG anodes at 400 mA g⁻¹ under cutoff capacity of 1000 mAh g⁻¹. Reproduced with permission from Ref. [202], Copyright 2019, American Chemical Society. (f) HRTEM image of Li₃P protective layer. (g) Photograph of *exsitu* electrolytes and Li anodes achieved after 100 cycles. (h) Cycling performance and discharge-charge potential plots for (i) Li₃P/Li anode. Reproduced with permission from Ref. [204], Copyright 2018, American Chemical Society.

Li-oxides and Li-S batteries, are not completely appropriate for Li-O₂ batteries operated in semi-open system [191]. Obviously, a typical excellent Li anode of Li-O₂ batteries needs to be dendrite-free, inert to electrolytes and contaminants, and volume-invariant.

Recently, 2D materials have shown unique advantages in protecting Li anodes for Li-O₂ batteries, and their major advances include two aspects of constructing stable SEI and porous host for Li anodes [192–195].

3.3.1. 2D materials for stable SEI

In 1979, Peled first proposed the concept of SEI film, immediately produced by the reaction of the active metal (*i.e.*, Li, Na) with the electrolyte [196]. However, this unstable SEI film will consume the gradual decomposition of electrolyte, leading to the degradation of cyclability. Therefore, the construction of stable SEI films have attracted much attention. So far, great progresses have been achieved through *in situ* growth of SEI films by chemical or electrochemical process, and *exsitu* or artificial protective film utilizing atomic layer deposition or spin coating methods [197]. These formed SEI films on Li anode can not only greatly suppress or mitigate the side reaction of Li anode with electrolyte, but also significantly reduce the influence by contaminants (O₂, H₂O) from the air cathode. Specifically, *in situ* chemical SEI film is formed through the rapid reaction between additives in electrolyte and Li metal [198]. However, this approach is generally hard to control the thickness and composition of SEI film, but the electrochemi-

cal synthesis to some extent precisely tunes the SEI films. Another way of *exsitu* or artificial protective film is considered to be more robust than the former of *in situ* SEI owing to its strong coupling with Li metal [199]. Owing to the advantages of such as lithophilicity and mechanical flexibility, 2D materials such as graphene have been gradually used for the modification of Li metal anodes. It should be emphasized that the remarkable advancements have been reported on the protection of Li anode in the closed lithium metal batteries, *e.g.*, lithium-oxide and Li-S batteries, by graphene-based materials [200,201]. However, there are only a few works for Li anodes of Li-O₂ cells. As a typical example, Zhao et al. applied fluorinated graphene-modified Li anodes (LFG) for Li-O₂ batteries, which obtained significant enhancement on cycling stability [202]. As shown in Fig. 12a-e, compared to bare Li, LFG anode showed higher discharge capacity of 6520 mAh g⁻¹, more stable cycling (91 cycles) and narrower voltage polarization. Furthermore, it is evident that the improvement of cycling performance of Li anode by fluorinated graphene introduction via DFT calculation. What's more, graphene-based composites have also been employed in the protection of Li anodes. Typically, Sun et al. reported a high energy efficiency Li-O₂ cell, which contained a Li anode protected by graphene-polydopamine composite layer and an electrolyte with continuous RM [203]. In addition, other 2D materials have also been studied on Li anode protection. For instance, Lee et al. prepared a high crystallinity 2D phosphorene based derived protective layer on the Li anode *via* a simple spin-coating method (Fig. 12f-i) [204]. Notably, the thermodynamically stable Li₃P

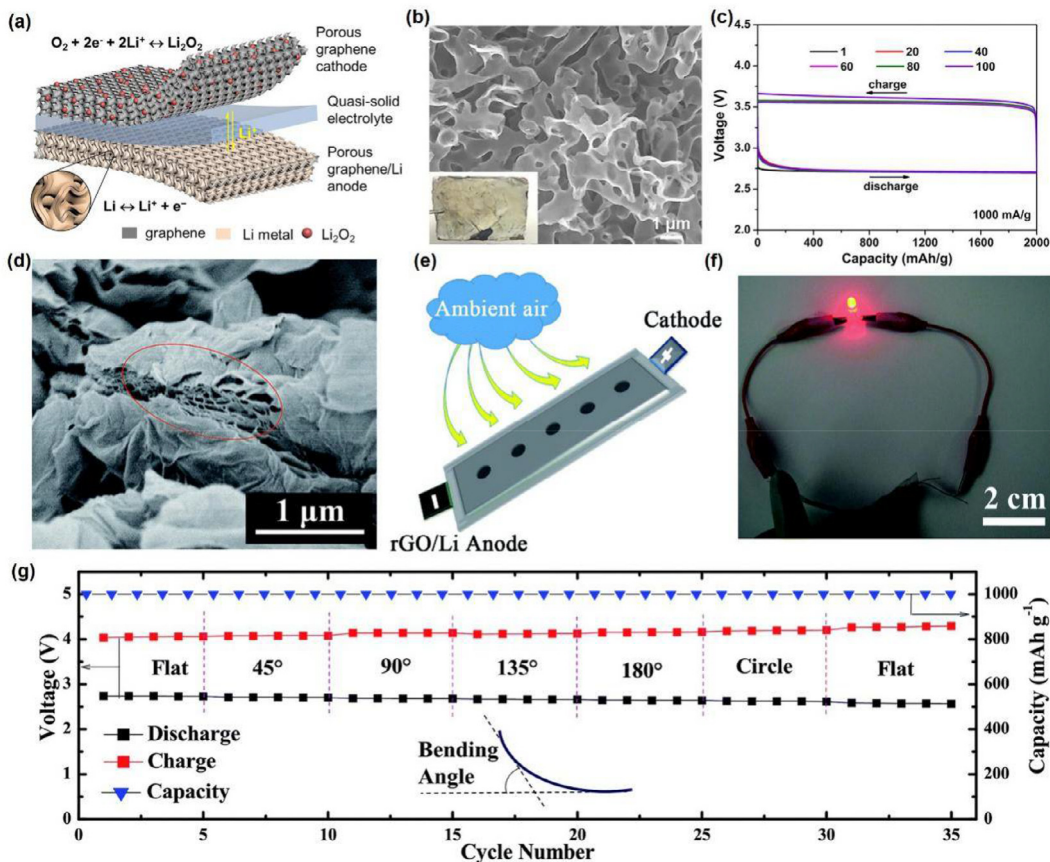


Fig. 13. (a) Schematic of a 3D porous graphene-based Li-O₂ cell. (b) SEM image and photograph of graphene-based Li anode. (c) Discharge/charge plots of porous graphene-based Li-O₂ cell at limited capacity of 2000 mAh g⁻¹. Reproduced with permission from Ref. [209]. Copyright 2018 from Ref. [209]. (d) SEM image of rGO membrane. (e) Schematic of a belt-shaped Li-air cell. (f) Photograph of a LED powered by a bent belt-shaped Li-air cell. (g) Cycling performance under different bending states tested under cutoff capacity of 1000 mAh g⁻¹ at 100 mA g⁻¹. Reproduced with permission from Ref. [211], Copyright 2018, Royal Society of Chemistry.

layer simultaneously restrained the decomposition of electrolyte and the growth of Li dendrites, which provided greatly enhanced cycling performance (over 50 cycles) in comparison with bare Li anode (10 cycles) in Li-O₂ batteries tested at 250 mA g⁻¹ under a constant capacity of 1000 mAh g⁻¹.

3.3.2. 2D materials as Li metal host

The SEI films can effectively prevent Li metal from direct contact with the electrolyte and contaminants in the surroundings to avoid the decomposition of electrolyte from and the growth of Li dendrites. However, the unstable SEI film cannot fundamentally inhibit the growth of Li dendrites during long-term cycle [197,205]. Moreover, the huge volume changes of Li anode in chemical or electrochemical processes must also be fully considered [206].

There are several theories about the growth of Li dendrites in lithium metal batteries [40]. It is generally accepted that the dendrites can be effectively suppressed by reducing the concentration of Li⁺ on surface. Based on this premise, using nanostructures as host for Li electrodes to dissipate the surface current density and simultaneously reduce the volume change of the electrode is a promising tactics to inhibit the Li dendrite [207,208]. For example, GO was incorporated into Li metal anode to achieve a metal-graphene scaffold due to its excellent Li affinity and wettability. As demonstrated, the as-obtained Li-GO electrode can successfully suppress the growth of Li metal dendrites and improve the cycling stability of Li metal battery. This strategy can remarkably increase the number of active sites and reduces local current density on Li anode.

There have been plentiful studies on 2D materials as porous matrix host for Li anodes in Li-S cells. However, only a few works of 2D materials-based Li anodes for Li-O₂ batteries were developed since 2D materials need to be precisely matched with the Li anode of Li-O₂ batteries. Typically, Chen et al. fabricated a rechargeable Li-O₂ battery, consisted of a Li-loaded 3D nanoporous graphene-based anode [209], gel/polymer electrolyte and a 3D porous graphene-based cathode, which showed outstanding performance with long cycle life over 100 cycles under limited capacity of 2000 mAh g⁻¹ at 1000 mA g⁻¹ (Fig. 13a-c).

Besides the conventional rigid cells, Li metal protection is particularly important in the progress of flexible Li metal-based batteries because the wrinkles or cracks formed during bending will result in a remarkable increase of the local Li⁺ concentration, which could give rise to the safety issue. As an example, The bending tolerant Li anode within 3D rGO scaffolds was explored by integrating Li metal into bendable frames of rGO film for flexible Li-O₂ batteries, demonstrative of prolong cycling stability [210]. In fact, the anode with 3D scaffolds simultaneously reduced the bending stress and increased specific surface area, when it was employed in nonaqueous Li-O₂ battery, a significant improvement of cycling performance more than 500 h under bending conditions was achieved. Furthermore, Feng et al. prepared a rGO based Li anode for the construction of a belt-shaped Li-air cell containing LiI and 4 wt% SiO₂ in gel/polymer electrolyte, which obtained long-term cycling for 100 cycles in ambient air [211]. As shown in Fig. 13d-g, the voltage plots were almost the same after bending different angles, indicating the excellent flexibility and stability of Li-air cell. Overall, the

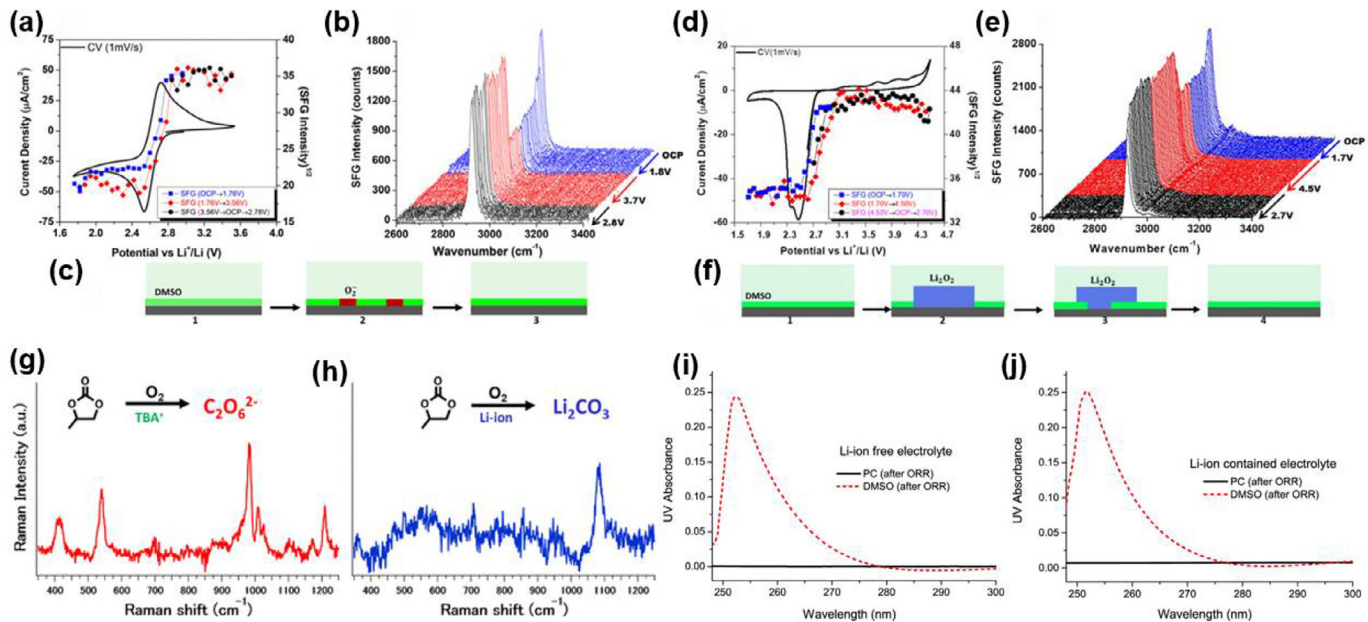


Fig. 14. (a) The CV curves of ORR/OER on a graphene cathode in 0.5 M O₂-saturated TBACIO₄/DMSO. (b) *In situ* SFG spectra continuously tested with the CV in (a). (c) Schematic model for the variation on the graphene surface from OCP to end of ORR and end of OER. (d) The CV curves of ORR/OER on a graphene cathode in 0.5 M O₂-saturated LiClO₄/DMSO. (e) *In situ* SFG spectra continuously tested with the CV of (d). (f) Schematic model for the variation on the graphene surface from OCP to end of ORR, middle and end of OER. Reproduced with permission from Ref. [224], Copyright 2018, American Chemical Society. (g) *In situ* SERS spectra on cathode in O₂-saturated 0.1 M TBACIO₄-based electrolyte during CV test. (h) *In situ* SERS spectra on cathode in O₂-saturated 0.1 M LiClO₄-based electrolyte during CV test. (i) *In situ* UV-vis spectra of 0.1 M TBACIO₄-PC and 0.1 M TBACIO₄-DMSO after ORR (j) *In situ* UV-vis spectra of 0.1 M LiClO₄-PC and 0.1 M LiClO₄-DMSO after ORR. Reproduced with permission from Ref. [225], Copyright 2020, American Chemical Society.

protection of Li metal anode plays a key role in stabilizing the anode and the whole battery, and it is highly expected that a long-term, dendrite-free Li-O₂ battery is realized by nanostructure engineering design of 2D materials.

3.4. Reaction mechanism of nonaqueous Li-O₂ batteries based on 2D materials

Although intensive researches have been focused on the improvement of cathodes, electrolytes, separators and anodes, the reaction mechanism, including ORR, the nucleation, growth, termination, decomposition of discharge products, Li dendrites and their impact on capacity fading and cycleability degradation in nonaqueous Li-O₂ batteries are still unclear, which subsequently hinder the rational design for Li-O₂ batteries to further improve the energy density and cycling stability [15,24]. Therefore, it is meaningful to explore the reaction mechanism for Li-O₂ batteries. In this regard, 2D materials with simple structure, high activity for ORR/OER and excellent stability are considered as ideal platform to deeply understand the reaction mechanism of Li-O₂ batteries in both theory and experiment [176].

For instance, Lei et al. systematically investigated the decomposition process of Li₂O₂ molecule on pristine graphene (G) and boron-doped graphene (BG) with first-principles calculation, revealing that two-step dissociation processes with the LiO₂ as reactive intermediate was advantageous over one-step dissociation processes [212]. As to another reaction of ORR, Kislenko et al. studied the behavior of Li⁺ and O₂ near the multi-layer graphene edge during discharging by molecular dynamics simulation, and found that the graphene edges might be the nucleation centers of discharge products due to the concentration of Li⁺ and O₂ reaching maximum [213].

Besides theoretical studies to understand the reaction mechanism on molecular/atom scale, developing advanced characterization techniques, including *exsitu* and *in situ* methods, for Li-O₂ batteries can more efficiently address the challenging issues in actual environment. As a typical example, the needle- or rod-like morphology of discharge prod-

ucts on Ir/rGO, which was different from the toroids and particles on rGO, were observed by SEM images. The phases of discharge products, LiO₂ and/or Li₂O₂, were identified by ex-situ XRD pattern, Raman, electron paramagnetic resonance (EPR) and TEM, which confirmed that the only LiO₂ formed on Ir/rGO through one-electron discharge process [33]. Similarly, Wunderlich et al. studied the mechanism of Li-O₂ batteries with graphite nanosheets as cathode by disassembling the cell in different depths of discharge. A distinctive two-step discharge behavior was validated with *exsitu* SEM and electrochemical impedance spectroscopy (EIS) characterization [214]. Different from *exsitu* characterization, *in situ*/operando characterization techniques can obtain the real-time information when the reactions of Li-O₂ batteries are in process [192]. Such *in situ* characterization techniques to explore the reaction mechanism include surface enhanced Raman spectroscopy (SERS) to probe the polarizable species on surface [215], SEM/TEM/AFM to unveil the morphology of the discharge products or charged species [216–218], EPR spectroscopy to detect the reactive species with unpaired electrons [219], XRD pattern to qualitatively and quantificationally analysis the discharge products/by-products [220], XPS to probe the chemical state of the Li-O₂ reaction intermediates on the surface [221], DEMS to monitor the gas consumption and evolution during cycling [222], ultraviolet-visible (UV-vis) spectroscopy to detect the solvated O₂[·] at around 252 nm during ORR and OER [223], sum frequency generation (SFG) vibrational spectroscopy to detect the molecular structures on a surface and/or interface [224]. These advanced techniques provide more direct and real-time evidences to reveal the reaction mechanism of Li-O₂ batteries. For example, Ji et al. revealed the origin of the high OER overpotential on a well-defined graphene cathode with *in situ* SFG spectroscopy shown in Fig. 14a-f, and found that the Li₂O₂ preferentially decomposed at the interface between the Li₂O₂ and graphene, thus the remained Li₂O₂ falling away from the conductive cathode increased the OER overpotential [224]. Further, several *in situ* characterization techniques working together could provide more direct information. As reported by Ye et al., the combination of SFG vibrational

spectroscopy, SERS and UV-vis was used to systematically investigate the degraded mechanism of the typical aprotic solvent dimethyl sulfoxide (DMSO) during ORR (Fig. 14g-j). It was proved that the by-products, Li_2CO_3 , was formed on the surface of graphene monolayer or thin gold film during ORR, which confirmed the decomposition of DMSO [225].

4. Summary and perspectives

In summary, we present a topic review on the key challenges and recent advances of 2D materials for high-energy-density nonaqueous Li-O_2 batteries, in which 2D materials can serve as multi-functional roles in the design of advanced cathodes, construction of solid-state electrolytes and separators, and protection of Li anodes. Special emphasis is given to 2D materials based oxygen cathodes, which can not only act as highly active oxygen electrocatalysts to boost the sluggish ORR and OER, but also serve as the conductive, porous oxygen electrodes to facilitate the transfer of both electrons and mass, furnish enough accommodation space for discharge products. Additionally, 2D materials modified separators and solid-state electrolytes can boost ionic mobility, fast redox reaction, and suppress the dendrite formation and growth. More importantly, 2D materials as coating layer and host of Li anodes can effectively prevent the Li dendrites during plating and stripping. In short, the state-of-the-art 2D materials employed in nonaqueous Li-O_2 batteries play a crucial role in improving energy density, round-trip efficiency, rate capability, cycling stability, safety and flexibility. Despite of the great advances, there are still several challenging issues unsolved on 2D materials for nonaqueous Li-O_2 batteries so far.

First, the exploration of highly active 2D materials-based air-cathodes with large storage capability is the key to construct high-performance Li-O_2 batteries. The design of novel oxygen cathodes with 2D materials are mainly involving three directions: (i) Construction of 3D porous networks derived from the assembly of 2D materials to provide multiple pathway for electron, oxygen, and Li^+ and supply storage space for discharge products; (ii) Introduction of dopants, defects, and other active phases into 2D materials for improving catalytic activity of ORR and OER; (iii) Creation of hierarchically structured 2D-1D system or tunable multilayer structure for increasing the storage capacity of lithium oxides and the contact range between electrolyte and air cathode. In particular, graphene-based materials can display high capacity by coupling with various active materials, and serve as the very competitive candidates of cathode materials for Li-O_2 cells. Besides, 2D TMOs/TMNs, TMCs and other 2D materials (e.g., MXene, phosphorene) are becoming a highly promising class of cathodes because of their abundant and controllable active phases for ORR/OER. Rational design and controllable fabrication of 2D heterostructures that combine the synergistic advantages of two different nanosheets, single/dual atom catalysts or nanosized alloys supported on 2D materials would be a reliable way to maximize the ORR/OER performance in cathode, and thus efficiently improve discharge/charge capacity, round-trip efficiency, rate capacity and cycling life for nonaqueous Li-O_2 batteries.

Second, rational screening of suitable 2D materials for solid-state electrolytes, separators and Li anodes is greatly significant to optimize the performance of Li-O_2 batteries. Solid-state electrolyte has been considered as the most effective candidates to obtain real Li-O_2 batteries because it can block contaminants from the air. However, its low ionic conductivity greatly limits its development. It is anticipated that the addition of 2D ionic conductive materials into solid-state electrolyte can enhance the intrinsic ionic conductivity, and meanwhile suppress the Li metal dendrites growth. Similarly, the separators constructed by 2D materials would display improved performance in safety and stability for Li-O_2 cells. The modification of Li anodes includes the interfacial construction of an artificial protective SEI film by covering 2D materials on the surface of Li anodes physically or chemically, and the elaborated design of 2D materials host Li anodes, while suppressing the decomposition of the electrolyte and growth of Li dendrites.

Third, the full consideration and systemic optimization of all the key devices components, e.g., cathode, electrolyte, and anode, as well as the interfacial matching should be taken into full consideration for the construction of a practical rechargeable Li-O_2 cells. The desirable approach to improve the performance of the whole device of Li-O_2 batteries involves the design of oxygen cathode catalysts and structures, selection of solid-state electrolytes and high-efficiency separators, and construction of dendritic-free Li anodes. Specifically, (i) designed construction of spatial structure air cathode (e.g., 1D-2D, 2D-2D) should meet the comprehensive requirements, such as high activity, outstanding electron-ion conductivity, large storage space, and high surface area for discharge products and electrolyte diffusion; (ii) Designed fabrication of a highly ionic conductive solid-state electrolyte or a highly selective separator using 2D materials, for example, BN, C_3N_4 , covalent organic frameworks, should combine the improvement on ionic conductivity, inhibition of the contaminants through them, and dissipation of interfacial resistance with air cathode and anode; (iii) Nanostructure engineering of stable SEI film and Li metal anode should consider 2D nanomaterials with lithophilic property and Young's modulus, which are of importance to inhibit Li dendrites and ease adverse reaction between Li anode and electrolyte. It is worth noting that the reported Li anode engineering strategies applied for other Li metal batteries can be employed in Li-O_2 batteries. For instance, using 3D skeletons of lithophilic nanosheets to host Li metal can be extended to produce a dendrite-free and stable Li anode for high-safe and high-energy-density Li-O_2 cells. Possibly, 2D materials could act as a low-lattice-mismatch substrate for the uniform electrodeposition of Li metal with thin-film structure, similar to the electrodeposition of Zn thin films on graphene [226].

Last but not least, advanced *in situ*/operando characterization technologies combined with theoretical models in Li-air batteries should also be valued, which can directly observe the structural evolution of both cathode and anodes during charging and discharging process, and achieve a deeper understanding of reaction intermediates, reaction process and reaction mechanism. What's more, it is believed that the in-depth fundamental understanding can provide reliable guidelines for designing and optimizing the key components for the performance enhancement of the whole device. Currently, *in situ* electron energy loss spectroscopy (EELS) has been employed to study the discharge products of Li-O_2 batteries [227], and *in situ* Raman spectroscopy has been well developed for probing the reaction intermediates and the influence of solvent in Li-O_2 batteries [228]. Besides, other characterization techniques (i.e., electron paramagnetic resonance) were also employed to investigate the OER/ORR mechanisms of Li-O_2 batteries [229]. Particularly, the *in situ* characterization techniques applied in other systems such as Li-S batteries can be employed in Li-O_2 batteries. For instance, *in situ* ultraviolet-visible (UV-vis) spectroscopy has been developed for detecting the intermediates of polysulfides [230].

In brief, 2D materials show great potential in performance enhancement of nonaqueous Li-O_2 batteries, and more importantly, 2D materials possess unique advantages in material design, system optimization, device modeling, and mechanism characterization owing to their ultrathin structure and exceptional physiochemical properties. Therefore, with the in-depth study and full understanding of their potential, it is anticipated that the 2D materials-based Li-O_2 batteries with high energy density, high power density, exceptional safety, and other smart functionality, e.g., flexibility for long-range electrical vehicles and convenient portable electronic devices can come true in the near future.

Declaration of Competing Interest

There are no conflicts to declare.

Acknowledgements

This work was financially supported by the National Key R&D Program of China (Grants 2016YBF0100100, and 2016YFA0200200),

National Natural Science Foundation of China (Grants 51872283, and 21805273), Liaoning BaiQianWan Talents Program, LiaoNing Revitalization Talents Program (Grant XLYC1807153), **Natural Science Foundation of Liaoning Province** (Grant 20180510038), **DICP** (DICP ZZBS201708, DICP ZZBS201802, and DICP I202032), **DICP&QIBEBT** (Grant DICP&QIBEBT UN201702), Dalian National Laboratory For Clean Energy (DNL), CAS, DNL Cooperation Fund, CAS (DNL180310, DNL180308, DNL201912, and DNL201915).

References

- [1] S.H. Ahn, X. Yu, A. Manthiram, “Wiring” Fe-N_x-embedded porous carbon framework onto 1D nanotubes for efficient oxygen reduction reaction in alkaline and acidic media, *Adv. Mater.* 29 (2017) 1606534.
- [2] Y. Tong, P. Chen, T. Zhou, K. Xu, W. Chu, C. Wu, Y. Xie, A bifunctional hybrid electrocatalyst for oxygen reduction and evolution: cobalt oxide nanoparticles strongly coupled to B,N-decorated graphene, *Angew. Chem. Int. Ed.* 56 (2017) 7121–7125.
- [3] H. Huang, F. Zhou, X. Shi, J. Qin, Z. Zhang, X. Bao, Z.-S. Wu, Graphene aerogel derived compact films for ultrafast and high-capacity aluminum ion batteries, *Energy Storage Mater.* 23 (2019) 664–669.
- [4] Y. Dong, Y. Li, H. Shi, J. Qin, S. Zheng, R. He, Z.-S. Wu, Graphene encapsulated iron nitrides confined in 3D carbon nanosheet frameworks for high-rate lithium ion batteries, *Carbon* 159 (2020) 213–220.
- [5] H.-F. Wang, C. Tang, Q. Zhang, A review of precious-metal-free bifunctional oxygen electrocatalysts: rational design and applications in Zn-air batteries, *Adv. Funct. Mater.* 28 (2018) 1803329.
- [6] A.P. Tiwari, D. Kim, Y. Kim, H. Lee, Bifunctional oxygen electrocatalysis through chemical bonding of transition metal chalcogenides on conductive carbons, *Adv. Energy Mater.* 7 (2017) 1602217.
- [7] X. Shi, S. Pei, F. Zhou, W. Ren, H.-M. Cheng, Z.-S. Wu, X. Bao, Ultrahigh-voltage integrated micro-supercapacitors with designable shapes and superior flexibility, *Energy Environ. Sci.* 12 (2019) 1534–1541.
- [8] S. Zheng, X. Shi, P. Das, Z.-S. Wu, X. Bao, The road towards planar microbatteries and micro-supercapacitors: from 2D to 3D device geometries, *Adv. Mater.* 31 (2019) 1900583.
- [9] N. Nitta, F. Wu, J.T. Lee, G. Yushin, Li-ion battery materials: present and future, *Mater. Today* 18 (2015) 252–264.
- [10] J.B. Goodenough, K.-S. Park, The Li-ion rechargeable battery: a perspective, *J. Am. Chem. Soc.* 135 (2013) 1167–1176.
- [11] V. Etacheri, R. Marom, R. Elazari, G. Salitra, D. Aurbach, Challenges in the development of advanced Li-ion batteries: a review, *Energy Environ. Sci.* 4 (2011) 3243–3262.
- [12] J.B. Goodenough, Y. Kim, Challenges for rechargeable Li batteries, *Chem. Mater.* 22 (2010) 587–603.
- [13] P.G. Bruce, S.A. Freunberger, L.J. Hardwick, J.-M. Tarascon, Li-O₂ and Li-S batteries with high energy storage, *Nat. Mater.* 11 (2012) 19–29.
- [14] L. Liu, H. Guo, L. Fu, S. Chou, S. Thiele, Y. Wu, J. Wang, Critical advances in ambient air operation of nonaqueous rechargeable Li-air batteries, *Small* (2019) e1903854.
- [15] W.J. Kwak, Rosy, D. Sharon, C. Xia, H. Kim, L.R. Johnson, P.G. Bruce, L.F. Nazar, Y.K. Sun, A.A. Frimer, M. Noked, S.A. Freunberger, D. Aurbach, Lithium-oxygen batteries and related systems: potential, status, and future, *Chem. Rev.* (2020), doi:10.1021/acs.chemrev.9b00609.
- [16] Y. Sun, N. Liu, Y. Cui, Promises and challenges of nanomaterials for lithium-based rechargeable batteries, *Nat. Energy* 1 (2016) 16071.
- [17] M.M.O. Thotiyil, S.A. Freunberger, Z. Peng, Y. Chen, Z. Liu, P.G. Bruce, A stable cathode for the aprotic Li-O₂ battery, *Nat. Mater.* 12 (2013) 1049–1055.
- [18] Y.-C. Lu, B.M. Gallant, D.G. Kwabi, J.R. Harding, R.R. Mitchell, M.S. Whittingham, Y. Shao-Horn, Lithium-oxygen batteries: bridging mechanistic understanding and battery performance, *Energy Environ. Sci.* 6 (2013) 750–768.
- [19] Z. Ma, X. Yuan, L. Li, Z.-F. Ma, D.P. Wilkinson, L. Zhang, J. Zhang, A review of cathode materials and structures for rechargeable lithium-air batteries, *Energy Environ. Sci.* 8 (2015) 2144–2198.
- [20] X. Guo, B. Sun, D. Su, X. Liu, H. Liu, Y. Wang, G. Wang, Recent developments of aprotic lithium-oxygen batteries: functional materials determine the electrochemical performance, *Sci. Bull.* 62 (2017) 442–452.
- [21] D. Wittmaier, N. Wagner, K.A. Friedrich, H.M.A. Amin, H. Baltruschat, Modified carbon-free silver electrodes for the use as cathodes in lithium-air batteries with an aqueous alkaline electrolyte, *J. Power Sources* 265 (2014) 299–308.
- [22] P. Zhang, H. Wang, Y.-G. Lee, M. Matsui, Y. Takeda, O. Yamamoto, N. Imanishi, Tape-cast water-stable NASICON-type high lithium ion conducting solid electrolyte films for aqueous lithium-air batteries, *J. Electrochem. Soc.* 162 (2015) A1265–A1271.
- [23] N. Alias, A.A. Mohamad, Advances of aqueous rechargeable lithium-ion battery: a review, *J. Power Sources* 274 (2015) 237–251.
- [24] T. Liu, J.P. Vivek, E.W. Zhao, J. Lei, N. Garcia-Araez, C.P. Grey, Current challenges and routes forward for nonaqueous lithium-air batteries, *Chem. Rev.* (2020), doi:10.1021/acs.chemrev.9b00545.
- [25] E.L. Littauer, K.C. Tsai, Anodic behavior of lithium in aqueous-electrolytes. 1. Transient passivation, *J. Electrochem. Soc.* 123 (1976) 771–776.
- [26] K.M. Abraham, Z. Jiang, A polymer electrolyte-based rechargeable lithium/oxygen battery, *J. Electrochem. Soc.* 143 (1996) 1–5.
- [27] C.O. Laoire, S. Mukerjee, K.M. Abraham, E.J. Plichta, M.A. Hendrickson, Elucidating the mechanism of oxygen reduction for lithium-air battery applications, *J. Phys. Chem. C* 113 (2009) 20127–20134.
- [28] C.O. Laoire, S. Mukerjee, K.M. Abraham, E.J. Plichta, M.A. Hendrickson, Influence of nonaqueous solvents on the electrochemistry of oxygen in the rechargeable lithium-air battery, *J. Phys. Chem. C* 114 (2010) 9178–9186.
- [29] J. Xiao, D. Mei, X. Li, W. Xu, D. Wang, G.L. Graff, W.D. Bennett, Z. Nie, L.V. Saraf, I.A. Aksay, J. Liu, J.-G. Zhang, Hierarchically porous graphene as a lithium-air battery electrode, *Nano Lett.* 11 (2011) 5071–5078.
- [30] Z. Peng, S.A. Freunberger, Y. Chen, P.G. Bruce, A reversible and higher-rate Li-O₂ battery, *Science* 337 (2012) 563–566.
- [31] Y. Chen, S.A. Freunberger, Z. Peng, O. Fontaine, P.G. Bruce, Charging a Li-O₂ battery using a redox mediator, *Nat. Chem.* 5 (2013) 489–494.
- [32] T. Liu, Q.-C. Liu, J.-J. Xu, X.-B. Zhang, Cable-type water-survivable flexible Li-O₂ battery, *Small* 12 (2016) 3101–3105.
- [33] J. Lu, Y.J. Lee, X. Luo, K.C. Lau, M. Asadi, H.-H. Wang, S. Brombosz, J. Wen, D. Zhai, Z. Chen, D.J. Miller, Y.S. Jeong, J.-B. Park, Z.Z. Fang, B. Kumar, A. Salehi-Khojin, Y.-K. Sun, L.A. Curtiss, K. Amine, A lithium-oxygen battery based on lithium superoxide, *Nature* 529 (2016) 377–382.
- [34] L. Luo, B. Liu, S. Song, W. Xu, J.-G. Zhang, C. Wang, Revealing the reaction mechanisms of Li-O₂ batteries using environmental transmission electron microscopy, *Nat. Nanotechnol.* 12 (2017) 535–539.
- [35] C. Xia, C.Y. Kwok, L.F. Nazar, A high-energy-density lithium-oxygen battery based on a reversible four-electron conversion to lithium oxide, *Science* 361 (2018) 777–781.
- [36] Y. Qiao, K. Jiang, H. Deng, H. Zhou, A high-energy-density and long-life lithium-ion battery via reversible oxide-peroxide conversion, *Nat. Catal.* 2 (2019) 1035–1044.
- [37] E.L. Littauer, K.C. Tsai, Anodic behavior of lithium in aqueous-electrolytes. 2. Mechanical passivation, *J. Electrochem. Soc.* 123 (1976) 964–969.
- [38] T. Liu, M. Leskes, W. Yu, A.J. Moore, L. Zhou, P.M. Bayley, G. Kim, C.P. Grey, Cycling Li-O batteries via LiOH formation and decomposition, *Science* 350 (2015) 530–533.
- [39] A. Dai, Q. Li, T. Liu, K. Amine, J. Lu, Fundamental understanding of water-induced mechanisms in Li-O₂ batteries: recent developments and perspectives, *Adv. Mater.* 31 (2019) e1805602.
- [40] D. Wang, W. Zhang, W. Zheng, X. Cui, T. Rojo, Q. Zhang, Towards high-safe lithium metal anodes: suppressing lithium dendrites via tuning surface energy, *Adv. Sci.* 4 (2017) 1600168.
- [41] R. Rojaee, R. Shahbazian-Yassar, Two dimensional materials to address the lithium battery challenges, *ACS Nano* 14 (2020) 2628–2658.
- [42] F. Su, X. Hou, J. Qin, Z.-S. Wu, Recent advances and challenges of two-dimensional materials for high-energy and high-power lithium-ion capacitors, *Batteries Supercaps* 3 (2020) 10–29.
- [43] E. Pomerantseva, Y. Gogotsi, Two-dimensional heterostructures for energy storage, *Nat. Energy* 2 (2017) 17089.
- [44] H. Tian, Z.W. Seh, K. Yan, Z. Fu, P. Tang, Y. Lu, R. Zhang, D. Legut, Y. Cui, Q. Zhang, Theoretical investigation of 2D layered materials as protective films for lithium and sodium Metal anodes, *Adv. Energy Mater.* 7 (2017) 1602528.
- [45] L. Shi, T. Zhao, Recent advances in inorganic 2D materials and their applications in lithium and sodium batteries, *J. Mater. Chem. A* 5 (2017) 3735–3758.
- [46] C. Zhang, A. Wang, J. Zhang, X. Guan, W. Tang, J. Luo, 2D Materials for lithium/sodium metal anodes, *Adv. Energy Mater.* 8 (2018) 1–13.
- [47] A. Raja, A. Chaves, J. Yu, G. Arefe, H.M. Hill, A.F. Rigosi, T.C. Berkelbach, P. Nagler, C. Schueler, T. Korn, C. Nuckolls, J. Hone, L.E. Brus, T.F. Heinz, D.R. Reichman, A. Chernikov, Coulomb engineering of the bandgap and excitons in two-dimensional materials, *Nat. Commun.* 8 (2017) 1–7.
- [48] C. Zhang, H. Huang, X. Ni, Y. Zhou, L. Kang, W. Jiang, H. Chen, J. Zhong, F. Liu, Band gap reduction in van der Waals layered 2D materials via a de-charge transfer mechanism, *Nanoscale* 10 (2018) 16759–16764.
- [49] Z.A. Ghazi, X. He, A.M. Khattak, N.A. Khan, B. Liang, A. Iqbal, J. Wang, H. Sin, L. Li, Z. Tang, Mo₂/celgard separator as efficient polysulfide barrier for long-life lithium-sulfur batteries, *Adv. Mater.* 29 (2017) 1–6.
- [50] P. Luo, F. Zhuge, Q. Zhang, Y. Chen, L. Lv, Y. Huang, H. Li, T. Zhai, Doping engineering and functionalization of two-dimensional metal chalcogenides, *Nanoscale Horiz.* 4 (2019) 26–51.
- [51] D. Akinwande, C.J. Brennan, J.S. Bunch, P. Egberts, J.R. Felts, H. Gao, R. Huang, J.-S. Kim, T. Li, Y. Li, K.M. Liechti, N. Lu, H.S. Park, E.J. Reed, P. Wang, B.I. Yakobson, T. Zhang, Y.-W. Zhang, Y. Zhou, Y. Zhu, A review on mechanics and mechanical properties of 2D materials-graphene and beyond, *Extreme Mech. Lett.* 13 (2017) 42–77.
- [52] Y. Hu, T. Zhang, F. Cheng, Q. Zhao, X. Han, J. Chen, Recycling application of Li-MnO₂ batteries as rechargeable lithium-air batteries, *Angew. Chem. Int. Ed.* 54 (2015) 4338–4343.
- [53] X. Lin, R. Yuan, Y. Cao, X. Ding, S. Cai, B. Han, Y. Hong, Z. Zhou, X. Yang, L. Gong, M. Zheng, Q. Dong, Controlling reversible expansion of Li₂O₂ formation and decomposition by modifying electrolyte in Li-O₂ batteries, *Chem* 4 (2018) 2685–2698.
- [54] C. Shu, J. Wang, J. Long, H.K. Liu, S.X. Dou, Understanding the reaction chemistry during charging in aprotic lithium-oxygen batteries: existing problems and solutions, *Adv. Mater.* 31 (2019) 1804587.
- [55] P. Zhang, Y. Zhao, X. Zhang, Functional and stability orientation synthesis of materials and structures in aprotic Li-O₂ batteries, *Chem. Soc. Rev.* 47 (2018) 2921–3004.
- [56] S. Yang, P. He, H. Zhou, Research progresses on materials and electrode design towards key challenges of Li-air batteries, *Energy Storage Mater.* 13 (2018) 29–48.

- [57] Y. Huang, Y. Wang, C. Tang, J. Wang, Q. Zhang, Y. Wang, J. Zhang, Atomic modulation and structure design of carbons for bifunctional electrocatalysis in metal-air batteries, *Adv. Mater.* 31 (2019) e1803800.
- [58] C. Chen, S. Xu, Y. Kuang, W. Gan, J. Song, G. Chen, G. Pastel, B. Liu, Y. Li, H. Huang, L. Hu, Nature-inspired tri-pathway design enabling high-performance flexible Li-O₂ batteries, *Adv. Energy Mater.* 9 (2019) 1802964.
- [59] X. Lin, R. Yuan, S. Cai, Y. Jiang, J. Lei, S.-G. Liu, Q.-H. Wu, H.-G. Liao, M. Zheng, Q. Dong, An open-structured matrix as oxygen cathode with high catalytic activity and large Li₂O₂ accommodations for lithium-oxygen batteries, *Adv. Energy Mater.* 8 (2018) 180089.
- [60] W. Yao, Y. Yuan, G. Tan, C. Liu, M. Cheng, V. Yurkiv, X. Bi, F. Long, C.R. Friedrich, F. Mashayek, K. Amine, J. Lu, R. Shahbazian-Yassar, Tuning Li₂O₂ formation routes by facet engineering of MnO₂ cathode catalysts, *J. Am. Chem. Soc.* 141 (2019) 12832–12838.
- [61] C. Zhao, C. Yu, M.N. Banis, Q. Sun, M. Zhang, X. Li, Y. Liu, Y. Zhao, H. Huang, S. Li, X. Han, B. Xiao, Z. Song, R. Li, J. Qiu, X. Sun, Decoupling atomic-layer-deposition ultrafine RuO₂ for high-efficiency and ultralong-life Li-O₂ batteries, *Nano Energy* 34 (2017) 399–407.
- [62] Y. Tu, D. Deng, X. Bao, Nanocarbons and their hybrids as catalysts for non-aqueous lithium-oxygen batteries, *J. Energy Chem.* 25 (2016) 957–966.
- [63] J. Lai, Y. Xing, N. Chen, L. Li, F. Wu, R. Chen, A comprehensive insight into the electrolytes for rechargeable lithium-air batteries, *Angew. Chem. Int. Ed.* 59 (2019) 2974–2997.
- [64] Z. Liu, J. Huang, Y. Zhang, B. Tong, F. Guo, J. Wang, Y. Shi, R. Wen, Z. Zhou, L. Guo, Z. Peng, Taming interfacial instability in lithium-oxygen batteries: a polymeric ionic liquid electrolyte solution, *Adv. Energy Mater.* 9 (2019) 1901967.
- [65] H. Zhang, G.G. Eshetu, X. Judez, C. Li, L.M. Rodriguez-Martinez, M. Armand, Electrolyte additives for lithium metal anodes and rechargeable lithium metal batteries: progress and perspectives, *Angew. Chem. Int. Ed.* 57 (2018) 15002–15027.
- [66] R. Black, B. Adams, L.F. Nazar, Non-aqueous and hybrid Li-O₂ batteries, *Adv. Energy Mater.* 2 (2012) 801–815.
- [67] H. Liao, H. Chen, F. Zhou, Z. Zhang, H. Chen, Dendrite-free lithium deposition induced by mechanical strong sponge-supported unique 3D cross-linking polymer electrolyte for lithium metal batteries, *J. Power Sources* 435 (2019) 226748.
- [68] I. Aldalur, M. Martinez-Ibanez, M. Piszcz, Z. Heng, M. Armand, Self-standing highly conductive solid electrolytes based on block copolymers for rechargeable all-solid-state lithium-metal batteries, *Batteries Supercaps* 1 (2018) 149–159.
- [69] A. Manthiram, X. Yu, S. Wang, Lithium battery chemistries enabled by solid-state electrolytes, *Nat. Rev. Mater.* 2 (2017) 16103.
- [70] J. Shim, H.J. Kim, B.G. Kim, Y.S. Kim, D.-G. Kim, J.-C. Lee, 2D boron nitride nanoflakes as a multifunctional additive in gel polymer electrolytes for safe, long cycle life and high rate lithium metal batteries, *Energy Environ. Sci.* 10 (2017) 1911–1916.
- [71] Y. Zhang, Y. Zhao, D. Gosselink, P. Chen, Synthesis of poly(ethylene-oxide)/nanoclay solid polymer electrolyte for all solid-state lithium/sulfur battery, *Ionics* 21 (2015) 381–385.
- [72] G. Jiang, S. Maeda, Y. Saito, S. Tanase, T. Sakai, Ceramic-polymer electrolytes for all-solid-state lithium rechargeable batteries, *J. Electrochem. Soc.* 152 (2005) A767–A773.
- [73] Y.-S. Ye, H. Wang, S.-G. Bi, Y. Xue, Z.-G. Xue, X.-P. Zhou, X.-L. Xie, Y.-W. Mai, High performance composite polymer electrolytes using polymeric ionic liquid-functionalized graphene molecular brushes, *J. Mater. Chem. A* 3 (2015) 18064–18073.
- [74] J. Yi, S. Guo, P. He, H. Zhou, Status and prospects of polymer electrolytes for solid-state Li-O₂ (air) batteries, *Energy Environ. Sci.* 10 (2017) 860–884.
- [75] X.B. Zhu, T.S. Zhao, Z.H. Wei, P. Tan, G. Zhao, A novel solid-state Li-O₂ battery with an integrated electrolyte and cathode structure, *Energy Environ. Sci.* 8 (2015) 2782–2790.
- [76] B. Kumar, J. Kumar, Cathodes for solid-state lithium-oxygen cells: roles of nasicon glass-ceramics, *J. Electrochem. Soc.* 157 (2010) A611–A616.
- [77] B. Kumar, J. Kumar, R. Leese, J.P. Fellner, S.J. Rodrigues, K.M. Abraham, A solid-state, rechargeable, long cycle life lithium-air battery, *J. Electrochem. Soc.* 157 (2010) A50–A54.
- [78] S.H. Lee, J.-B. Park, H.-S. Lim, Y.-K. Sun, An advanced separator for Li-O₂ batteries: maximizing the effect of redox mediators, *Adv. Energy Mater.* 7 (2017) 1602417.
- [79] B.G. Kim, J.-S. Kim, J. Min, Y.-H. Lee, J.H. Choi, M.C. Jang, S.A. Freunberger, J.W. Choi, A moisture and oxygen-impermeable separator for aprotic Li-O₂ batteries, *Adv. Funct. Mater.* 26 (2016) 1747–1756.
- [80] W. Luo, L. Zhou, K. Fu, Z. Yang, J. Wan, M. Manno, Y. Yao, H. Zhu, B. Yang, L. Hu, A thermally conductive separator for stable Li metal anodes, *Nano Lett.* 15 (2015) 6149–6154.
- [81] C.-N. Wei, C. Karuppiyah, C.-C. Yang, J.-Y. Shih, S.J. Lue, Bifunctional perovskite electrocatalyst and PVDF/PET/PVDF separator integrated split test cell for high performance Li-O₂ battery, *J. Phys. Chem. Solids* 133 (2019) 67–78.
- [82] J.-J. Xu, Q.-C. Liu, Y. Yu, J. Wang, J.-M. Yan, X.-B. Zhang, In situ construction of stable tissue-directed/reinforced bifunctional separator/protection film on lithium anode for lithium-oxygen batteries, *Adv. Mater.* 29 (2017) 1606552.
- [83] J.-K. Kim, D.H. Kim, S.H. Joo, B. Choi, A. Cha, K.M. Kim, T.-H. Kwon, S.K. Kwak, S.J. Kang, J. Jin, Hierarchical chitin fibers with aligned nanofibrillar architectures: a nonwoven-mat separator for lithium metal batteries, *ACS Nano* 11 (2017) 6114–6121.
- [84] S.H. Lee, J.R. Harding, D.S. Liu, J.M. D'Arcy, Y. Shao-Horn, P.T. Hammond, Li-anode protective layers for Li rechargeable batteries via layer-by-layer approaches, *Chem. Mater.* 26 (2014) 2579–2585.
- [85] H. Wang, M. Matsui, H. Kuwata, H. Sonoki, Y. Matsuda, X. Shang, Y. Takeda, O. Yamamoto, N. Imanishi, A reversible dendrite-free high-areal-capacity lithium metal electrode, *Nat. Commun.* 8 (2017) 15106.
- [86] D. Lin, Y. Liu, Y. Cui, Reviving the lithium metal anode for high-energy batteries, *Nat. Nanotechnol.* 12 (2017) 194–206.
- [87] Y. Guo, H. Li, T. Zhai, Reviving lithium-metal anodes for next-generation high-energy batteries, *Adv. Mater.* 29 (2017) 1700007.
- [88] A. Zhamu, G. Chen, C. Liu, D. Neff, Q. Fang, Z. Yu, W. Xiong, Y. Wang, X. Wang, B.Z. Jang, Reviving rechargeable lithium metal batteries: enabling next-generation high-energy and high-power cells, *Energy Environ. Sci.* 5 (2012) 5701–5707.
- [89] R. Pathak, K. Chen, A. Gurung, K.M. Reza, B. Bahrami, F. Wu, A. Chaudhary, N. Ghimire, B. Zhou, W.-H. Zhang, Y. Zhou, Q. Qiao, Ultrathin bilayer of graphite/SiO₂ as solid interface for reviving Li metal anode, *Adv. Energy Mater.* 9 (2019) 1901486.
- [90] R. Pan, R. Sun, Z. Wang, J. Lindh, K. Edstrom, M. Stromme, L. Nyholm, Sandwich-structured nano/micro fiber-based separators for lithium metal batteries, *Nano Energy* 55 (2019) 316–326.
- [91] W. Xu, J. Wang, F. Ding, X. Chen, E. Nasibutin, Y. Zhang, J.-G. Zhang, Lithium metal anodes for rechargeable batteries, *Energy Environ. Sci.* 7 (2014) 513–537.
- [92] G. Girishkumar, B. McCloskey, A.C. Luntz, S. Swanson, W. Wilcke, Lithium-air battery: promise and challenges, *J. Phys. Chem. Lett.* 1 (2010) 2193–2203.
- [93] D. Lin, Y. Liu, Z. Liang, H.-W. Lee, J. Sun, H. Wang, K. Yan, J. Xie, Y. Cui, Layered reduced graphene oxide with nanoscale interlayer gaps as a stable host for lithium metal anodes, *Nat. Nanotechnol.* 11 (2016) 626–632.
- [94] Z. Guo, F. Wang, Z. Li, Y. Yang, A.G. Tamirat, H. Qi, J. Han, W. Li, L. Wang, S. Feng, Lithophilic Co/Co₃N nanoparticles embedded in hollow N-doped carbon nanocubes stabilizing lithium metal anodes for Li-air batteries, *J. Mater. Chem. A* 6 (2018) 22092–22105.
- [95] C. Yan, X.B. Cheng, Y. Tian, X. Chen, X.Q. Zhang, W.J. Li, J.Q. Huang, Q. Zhang, Dual-layered film protected lithium metal anode to enable dendrite-free lithium deposition, *Adv. Mater.* 30 (2018) e1707629.
- [96] L. Ye, M. Liao, H. Sun, Y. Yang, C. Tang, Y. Zhao, L. Wang, Y. Xu, L. Zhang, B. Wang, F. Xu, X. Sun, Y. Zhang, H. Dai, P.G. Bruce, H. Peng, Stabilizing lithium into cross-stacked nanotube sheets with an ultra-high specific capacity for lithium oxygen batteries, *Angew. Chem. Int. Ed.* 58 (2019) 2437–2442.
- [97] B.G. Kim, C. Jo, J. Shin, Y. Mun, J. Lee, J.W. Choi, Ordered mesoporous titanium nitride as a promising carbon-free cathode for aprotic lithium-oxygen batteries, *ACS Nano* 11 (2017) 1736–1746.
- [98] B. Qiu, M. Xing, J. Zhang, Recent advances in three-dimensional graphene based materials for catalysis applications, *Chem. Soc. Rev.* 47 (2018) 2165–2216.
- [99] A.H. Khan, S. Ghosh, B. Pradhan, A. Dalui, L.K. Shrestha, S. Acharya, K. Ariga, Two-dimensional (2D) nanomaterials towards electrochemical nanoarchitectonics in energy-related applications, *Bull. Chem. Soc. Jpn.* 90 (2017) 627–648.
- [100] F. Bonaccorso, L. Colombo, G. Yu, M. Stoller, V. Tozzini, A.C. Ferrari, R.S. Ruoff, V. Pellegrini, Graphene, related two-dimensional crystals, and hybrid systems for energy conversion and storage, *Science* 347 (2015) 1246501.
- [101] Y. Sun, Q. Wu, G. Shi, Graphene based new energy materials, *Energy Environ. Sci.* 4 (2011) 1113–1132.
- [102] K.R. Paton, E. Varrla, C. Backes, R.J. Smith, U. Khan, A. O'Neill, C. Boland, M. Lotya, O.M. Istrate, P. King, T. Higgins, S. Barwick, P. May, P. Puczkarski, I. Ahmed, M. Moebius, H. Pettersson, E. Long, J. Coelho, S.E. O'Brien, E.K. McGuire, B.M. Sanchez, G.S. Duesberg, N. McEvoy, T.J. Pennycook, C. Downing, A. Crossley, V. Nicolosi, J.N. Coleman, Scalable production of large quantities of defect-free few-layer graphene by shear exfoliation in liquids, *Nat. Mater.* 13 (2014) 624–630.
- [103] J.N. Coleman, Liquid exfoliation of defect-free graphene, *Acc. Chem. Res.* 46 (2013) 14–22.
- [104] A. Sakhaei-Pour, M.T. Ahmadian, A. Vafai, Applications of single-layered graphene sheets as mass sensors and atomistic dust detectors, *Solid State Commun.* 145 (2008) 168–172.
- [105] Z. Chang, J. Xu, X. Zhang, Recent progress in electrocatalyst for Li-O₂ Batteries, *Adv. Energy Mater.* 7 (2017) 1700875.
- [106] D. Capsoni, M. Bini, S. Ferrari, E. Quartarone, P. Mustarelli, Recent advances in the development of Li-air batteries, *J. Power Sources* 220 (2012) 253–263.
- [107] B. Sun, X. Huang, S. Chen, P. Munroe, G. Wang, Porous graphene nanoarchitectures: an efficient catalyst for low charge-overpotential, long life, and high capacity lithium-oxygen batteries, *Nano Lett.* 14 (2014) 3145–3152.
- [108] Q. Li, P. Xu, W. Gao, S. Ma, G. Zhang, R. Cao, J. Cho, H.-L. Wang, G. Wu, Graphene/graphene-tube nanocomposites templated from cage-containing metal-organic frameworks for oxygen reduction in Li-O₂ batteries, *Adv. Mater.* 26 (2014) 1378–1386.
- [109] G. Wu, N.H. Mack, W. Gao, S. Ma, R. Zhong, J. Han, J.K. Baldwin, P. Zelenay, Nitrogen doped graphene-rich catalysts derived from heteroatom polymers for oxygen reduction in nonaqueous lithium-O₂ battery cathodes, *ACS Nano* 6 (2012) 9764–9776.
- [110] Q. Jia, S. Ghoshal, J. Li, W. Liang, G. Meng, H. Che, S. Zhang, Z.F. Ma, S. Mukerjee, Metal and metal oxide interactions and their catalytic consequences for oxygen reduction reaction, *J. Am. Chem. Soc.* 139 (2017) 7893–7903.
- [111] H.-G. Jung, Y.S. Jeong, J.-B. Park, Y.-K. Sun, B. Scrosati, Y.J. Lee, Ruthenium-based electrocatalysts supported on reduced graphene oxide for lithium-air batteries, *ACS Nano* 7 (2013) 3532–3539.
- [112] M. Nazarian-Samani, H.-D. Lim, S. Haghigat-Shishavan, H.-K. Kim, Y. Ko, M.-S. Kim, S.-W. Lee, S.F. Kashani-Bozorg, M. Abbasi, H.-U. Guim, D.-I. Kim, K.-C. Roh, K. Kang, K.-B. Kim, A robust design of Ru quantum dot/N-doped holey graphene for efficient Li-O₂ batteries, *J. Mater. Chem. A* 5 (2017) 619–631.
- [113] L. Leng, J. Li, X. Zeng, H. Song, T. Shu, H. Wang, S. Liao, Enhancing the cyclability of Li-O₂ batteries using PdM alloy nanoparticles anchored on nitrogen-doped reduced graphene as the cathode catalyst, *J. Power Sources* 337 (2017) 173–179.

- [114] Y. Tu, H. Li, D. Deng, J. Xiao, X. Cui, D. Ding, M. Chen, X. Bao, Low charge overpotential of lithium-oxygen batteries with metallic Co encapsulated in single-layer graphene shell as the catalyst, *Nano Energy* 30 (2016) 877–884.
- [115] S. Kumar, D. Kumar, P. Karunanithi, S. Kumar, M. Goswami, A. Singh, N. Singh, F. Alam, N. Sathish, D. Choudhary, M. Ashiq, Self-assembled nickel anchored reduced graphene oxide hybrids: synergistic performance of electro-catalyst for oxygen reduction reaction in non-aqueous medium, *Mater. Res. Express* 6 (2019) 125520.
- [116] M. Ren, J. Zhang, M. Fan, P.M. Ajayan, J.M. Tour, Li-breathing air batteries catalyzed by MnNiFe/laser-induced graphene catalysts, *Adv. Mater. Interfaces* 6 (2019) 1901035.
- [117] D.-S. Kim, G.-H. Lee, S. Lee, J.-C. Kim, H.J. Lee, B.-K. Kim, D.-W. Kim, Electrocatalytic performance of CuO/graphene nanocomposites for Li-O₂ batteries, *J. Alloys Compd.* 707 (2017) 275–280.
- [118] W.H. Ryu, T.H. Yoon, S.H. Song, S. Jeon, Y.J. Park, I.D. Kim, Bifunctional composite catalysts using Co₃O₄ nanofibers immobilized on nonoxidized graphene nanoflakes for high-capacity and long-cycle Li-O₂ batteries, *Nano Lett.* 13 (2013) 4190–4197.
- [119] G.-H. Lee, M.-C. Sung, J.-C. Kim, H.J. Song, D.-W. Kim, Synergistic effect of CuGeO₃/graphene composites for efficient oxygen-electrode electrocatalysts in Li-O₂ batteries, *Adv. Energy Mater.* 8 (2018) 1801930.
- [120] Q. Li, P. Xu, B. Zhang, H. Tsai, J. Wang, H.L. Wang, G. Wu, One-step synthesis of Mn₃O₄/reduced graphene oxide nanocomposites for oxygen reduction in nonaqueous Li-O₂ batteries, *Chem. Commun.* 49 (2013) 10838–10840.
- [121] K.H. Lim, S. Kim, H. Kweon, S. Moon, C.H. Lee, H. Kim, Preparation of graphene hollow spheres from vacuum residue of ultra-heavy oil as an effective oxygen electrode for Li-O₂ batteries, *J. Mater. Chem. A* 6 (2018) 4040–4047.
- [122] W. Zhang, J. Zhu, H. Ang, Y. Zeng, N. Xiao, Y. Gao, W. Liu, H.H. Hng, Q. Yan, Binder-free graphene foams for O₂ electrodes of Li-O₂ batteries, *Nanoscale* 5 (2013) 9651–9658.
- [123] C. Liu, R. Younesi, C.-W. Tai, M. Valvo, K. Edström, T. Gustafsson, J. Zhu, 3-D binder-free graphene foam as a cathode for high capacity Li-O₂ batteries, *J. Mater. Chem. A* 4 (2016) 9767–9773.
- [124] X. Zhong, B. Papandrea, Y. Xu, Z. Lin, H. Zhang, Y. Liu, Y. Huang, X. Duan, Three-dimensional graphene membrane cathode for high energy density rechargeable lithium-air batteries in ambient conditions, *Nano Res.* 10 (2016) 472–482.
- [125] C. Zhao, C. Yu, S. Liu, J. Yang, X. Fan, H. Huang, J. Qiu, 3D porous N-doped graphene frameworks made of interconnected nanocages for ultrahigh-rate and long-life Li-O₂ batteries, *Adv. Funct. Mater.* 25 (2015) 6913–6920.
- [126] F. Wu, Y. Xing, L. Li, J. Qian, W. Qu, J. Wen, D. Miller, Y. Ye, R. Chen, K. Amine, J. Lu, Facile synthesis of boron-doped rGO as cathode material for high energy Li-O₂ batteries, *ACS Appl. Mater. Interfaces* 8 (2016) 23635–23645.
- [127] J. Han, X. Guo, Y. Ito, P. Liu, D. Hojo, T. Aida, A. Hirata, T. Fujita, T. Adschari, H. Zhou, M. Chen, Effect of chemical doping on cathodic performance of bicontinuous nanoporous graphene for Li-O₂ batteries, *Adv. Energy Mater.* 6 (2016) 1501870.
- [128] X. Guo, P. Liu, J. Han, Y. Ito, A. Hirata, T. Fujita, M. Chen, 3D nanoporous nitrogen-doped graphene with encapsulated RuO₂ nanoparticles for Li-O₂ batteries, *Adv. Mater.* 27 (2015) 6137–6143.
- [129] P. Zhang, R. Wang, M. He, J. Lang, S. Xu, X. Yan, 3D hierarchical Co/CoO-graphene-carbonized melamine foam as a superior cathode toward long-life lithium oxygen batteries, *Adv. Funct. Mater.* 26 (2016) 1354–1364.
- [130] J. Zhu, M. Metzger, M. Antonietti, T.P. Fellinger, Vertically aligned two-dimensional graphene-metal hydroxide hybrid arrays for Li-O₂ batteries, *ACS Appl. Mater. Interfaces* 8 (2016) 26041–26050.
- [131] Z. Lyu, Y. Zhou, W. Dai, X. Cui, M. Lai, L. Wang, F. Huo, W. Huang, Z. Hu, W. Chen, Recent advances in understanding of the mechanism and control of Li₂O₂ formation in aprotic Li-O₂ batteries, *Chem. Soc. Rev.* 46 (2017) 6046–6072.
- [132] C. Yang, R.A. Wong, M. Hong, K. Yamanaka, T. Ohta, H.R. Byon, Unexpected Li₂O₂ film growth on carbon nanotube electrodes with CeO₂ nanoparticles in Li-O₂ batteries, *Nano Lett.* 16 (2016) 2969–2974.
- [133] Y. Zheng, R. Gao, L. Zheng, L. Sun, Z. Hu, X. Liu, Ultrathin Co₃O₄ nanosheets with edge-enriched {111} planes as efficient catalysts for lithium-oxygen batteries, *ACS Catal.* 9 (2019) 3773–3782.
- [134] C. Tang, P. Sun, J. Xie, Z. Tang, Z. Yang, Z. Dong, G. Cao, S. Zhang, P.V. Braun, X. Zhao, Two-dimensional IrO₂/MnO₂ enabling conformal growth of amorphous Li₂O₂ for high-performance Li-O₂ batteries, *Energy Storage Mater.* 9 (2017) 206–213.
- [135] T. Ogasawara, A. Debart, M. Holzapfel, P. Novak, P.G. Bruce, Rechargeable Li₂O₂ electrode for lithium batteries, *J. Am. Chem. Soc.* 128 (2006) 1390–1393.
- [136] A. Debart, A.J. Paterson, J. Bao, P.G. Bruce, Alpha-MnO nanowires: a catalyst for the O₂ electrode in rechargeable lithium batteries, *Angew. Chem. Int. Ed.* 47 (2008) 4521–4524.
- [137] L. Trahey, N.K. Karan, M.K.Y. Chan, J. Lu, Y. Ren, J. Greeley, M. Balasubramanian, A.K. Burrell, L.A. Curtiss, M.M. Thackeray, Synthesis, characterization, and structural modeling of high-capacity, dual functioning MnO₂ electrode/electrocatalysts for Li-O₂ cells, *Adv. Energy Mater.* 3 (2013) 75–84.
- [138] S. Chen, G. Liu, H. Yadegari, H. Wang, S.Z. Qiao, Three-dimensional MnO₂ ultrathin nanosheet aerogels for high-performance Li-O₂ batteries, *J. Mater. Chem. A* 3 (2015) 2559–2563.
- [139] Y.K. Jo, W. Tamakloe, X. Jin, J. Lim, S.B. Patil, Y.-M. Kang, S.-J. Hwang, Multilayer hybrid nanosheet of mesoporous carbon-layered metal oxide as a highly efficient electrocatalyst for Li-O₂ batteries, *Appl. Catal. B* 254 (2019) 523–530.
- [140] K. Adpakpang, S.M. Oh, D.A. Agyeman, X. Jin, N. Jarulertwathan, I.Y. Kim, T. Sarakonsri, Y.-M. Kang, S.-J. Hwang, Holey 2D nanosheets of low-valent manganese oxides with an excellent oxygen catalytic activity and a high functionality as a catalyst for Li-O₂ batteries, *Adv. Funct. Mater.* 28 (2018) 1707106.
- [141] C. Cao, J. Xie, S. Zhang, B. Pan, G. Cao, X. Zhao, Graphene-like δ-MnO₂ decorated with ultrafine CeO₂ as a highly efficient catalyst for long-life lithium-oxygen batteries, *J. Mater. Chem. A* 5 (2017) 6747–6755.
- [142] Z. Song, N. Cao, X. Gao, Q. Liang, X. Qin, Ultrathin Co₃O₄ nanosheets highly dispersed on reduced graphene oxide: an efficient bi-functional catalyst for Li-O₂ battery, *Fuller. Nanotubes Carbon Nanostruct.* 25 (2017) 65–70.
- [143] Y. Zhang, M. Hu, M. Yuan, G. Sun, Y. Li, K. Zhou, C. Chen, C. Nan, Y. Li, Ordered two-dimensional porous Co₃O₄ nanosheets as electrocatalysts for rechargeable Li-O₂ batteries, *Nano Res.* 12 (2018) 299–302.
- [144] S. Zhang, G. Wang, J. Jin, L. Zhang, Z. Wen, J. Yang, Self-catalyzed decomposition of discharge products on the oxygen vacancy sites of MoO₃ nanosheets for low-overpotential Li-O₂ batteries, *Nano Energy* 36 (2017) 186–196.
- [145] X. Cao, Z. Sun, X. Zheng, C. Jin, J. Tian, X. Li, R. Yang, MnCo₂O₄/MoO₂ nanosheets grown on Ni foam as carbon- and binder-free cathode for lithium-oxygen batteries, *ChemSusChem* 11 (2018) 574–579.
- [146] K. Liao, X. Wang, Y. Sun, D. Tang, M. Han, P. He, X. Jiang, T. Zhang, H. Zhou, An oxygen cathode with stable full discharge-charge capability based on 2D conducting oxide, *Energy Environ. Sci.* 8 (2015) 1992–1997.
- [147] J. Huang, Z. Jin, Z.-L. Xu, L. Qin, H. Huang, Z. Sadighi, S. Yao, J. Cui, B. Huang, J.-K. Kim, Porous RuO₂ nanosheet/CNT electrodes for DMSO-based Li-O₂ and Li ion O₂ batteries, *Energy Storage Mater.* 8 (2017) 110–118.
- [148] H.F. Wang, C. Tang, B. Wang, B.Q. Li, Q. Zhang, Bifunctional transition metal hydroxysulfides: room-temperature sulfurization and their applications in Zn-air batteries, *Adv. Mater.* 29 (2017) 1702327.
- [149] M. Yu, S. Zhou, Z. Wang, J. Zhao, J. Qiu, Boosting electrocatalytic oxygen evolution by synergistically coupling layered double hydroxide with MXene, *Nano Energy* 44 (2018) 181–190.
- [150] F. Li, J. Du, X. Li, J. Shen, Y. Wang, Y. Zhu, L. Sun, Integration of FeOOH and zeolitic imidazolate framework-derived nanoporous carbon as an efficient electrocatalyst for water oxidation, *Adv. Energy Mater.* 8 (2018) 1702598.
- [151] Q. Wang, L. Shang, R. Shi, X. Zhang, Y. Zhao, G.I.N. Waterhouse, L.-Z. Wu, C.-H. Tung, T. Zhang, NiFe layered double hydroxide nanoparticles on Co,N-codoped carbon nanoframes as efficient bifunctional catalysts for rechargeable zinc-air batteries, *Adv. Energy Mater.* 7 (2017) 1700467.
- [152] S. Chitravathi, S. Kumar, N. Munichandraiah, NiFe-layered double hydroxides: a bi-functional O₂ electrode catalyst for non-aqueous Li-O₂ batteries, *RSC Adv.* 6 (2016) 103106–103115.
- [153] S.-M. Xu, Q.-C. Zhu, J. Long, H.-H. Wang, X.-F. Xie, K.-X. Wang, J.-S. Chen, Low-overpotential Li-O₂ batteries based on TFSI intercalated Co-Ti layered double oxides, *Adv. Funct. Mater.* 26 (2016) 1365–1374.
- [154] X. Lu, N. Sakai, D. Tang, X. Li, T. Taniguchi, R. Ma, T. Sasaki, CoNiFe layered double hydroxide/RuO_{2,1} nanosheet superlattice as carbon-free electrocatalysts for water splitting and Li-O₂ batteries, *ACS Appl. Mater. Interfaces* (2020), doi:10.1021/acsm.acsapplimat.0c07656.
- [155] M. Asadi, B. Kumar, C. Liu, P. Phillips, P. Yasaee, A. Behranginia, P. Zapol, R.F. Klie, L.A. Curtiss, A. Salehi-Khojin, Cathode based on molybdenum disulfide nanoflakes for lithium-oxygen batteries, *ACS Nano* 10 (2016) 2167–2175.
- [156] Z. Sadighi, J. Liu, L. Zhao, F. Ciucci, J.K. Kim, Metallic MoS nanosheets: multifunctional electrocatalyst for the ORR, OER and Li-O₂ batteries, *Nanoscale* 10 (2018) 22549–22559.
- [157] Z. Sadighi, J. Liu, F. Ciucci, J.K. Kim, Mesoporous MnCo₂S₄ nanosheet arrays as an efficient catalyst for Li-O₂ batteries, *Nanoscale* 10 (2018) 15588–15599.
- [158] Y. Ji, H. Dong, M. Yang, T. Hou, Y. Li, Monolayer germanium monochalcogenides (GeS/GeSe) as cathode catalysts in nonaqueous Li-O₂ batteries, *Phys. Chem. Chem. Phys.* 19 (2017) 20457–20462.
- [159] J. Yi, K. Liao, C. Zhang, T. Zhang, F. Li, H. Zhou, Facile in situ preparation of graphitic-C₃N₄@carbon paper as an efficient metal-free cathode for nonaqueous Li-O₂ battery, *ACS Appl. Mater. Interfaces* 7 (2015) 10823–10827.
- [160] S. Liu, Z. Wang, S. Zhou, F. Yu, M. Yu, C.Y. Chiang, W. Zhou, J. Zhao, J. Qiu, Metal-organic-framework-derived hybrid carbon nanocages as a bifunctional electrocatalyst for oxygen reduction and evolution, *Adv. Mater.* 29 (2017) 1700874.
- [161] L. Shang, H. Yu, X. Huang, T. Bian, R. Shi, Y. Zhao, G.I. Waterhouse, L.Z. Wu, C.H. Tung, T. Zhang, Well-dispersed ZIF-derived Co,N-co-doped carbon nanoframes through mesoporous-silica-protected calcination as efficient oxygen reduction electrocatalysts, *Adv. Mater.* 28 (2016) 1668–1674.
- [162] M. Zhang, Q. Dai, H. Zheng, M. Chen, L. Dai, Novel MOF-derived Co@N-C bifunctional catalysts for highly efficient Zn-air batteries and water splitting, *Adv. Mater.* 30 (2018) 1705431.
- [163] M. Zhao, Y. Huang, Y. Peng, Z. Huang, Q. Ma, H. Zhang, Two-dimensional metal-organic framework nanosheets: synthesis and applications, *Chem. Soc. Rev.* 47 (2018) 6267–6295.
- [164] L. Zhao, B. Dong, S. Li, L. Zhou, L. Lai, Z. Wang, S. Zhao, M. Han, K. Gao, M. Lu, X. Xie, B. Chen, Z. Liu, X. Wang, H. Zhang, H. Li, J. Liu, H. Zhang, X. Huang, W. Huang, Interdiffusion reaction-assisted hybridization of two-dimensional metal-organic frameworks and Ti₃C₂T_x nanosheets for electrocatalytic oxygen evolution, *ACS Nano* 11 (2017) 5800–5807.
- [165] M. Zhao, Y. Wang, Q. Ma, Y. Huang, X. Zhang, J. Ping, Z. Zhang, Q. Lu, Y. Yu, H. Xu, Y. Zhao, H. Zhang, Ultrathin 2D metal-organic framework nanosheets, *Adv. Mater.* 27 (2015) 7372–7378.
- [166] A. Kondo, H. Noguchi, S. Ohnishi, H. Kajiro, A. Tohdoh, Y. Hattori, W.-C. Xu, H. Tanaka, H. Kanoh, K. Kaneko, Novel expansion/shrinkage modulation of 2D layered MOF triggered by clathrate formation with CO₂ molecules, *Nano Lett.* 6 (2006) 2581–2584.

- [167] M. Yuan, R. Wang, W. Fu, L. Lin, Z. Sun, X. Long, S. Zhang, C. Nan, G. Sun, H. Li, S. Ma, Ultrathin two-dimensional metal-organic framework nanosheets with the inherent open active sites as electrocatalysts in aprotic Li-O_2 batteries, *ACS Appl. Mater. Interfaces* 11 (2019) 11403–11413.
- [168] A. Togo, I. Tanaka, First principles phonon calculations in materials science, *Scr. Mater.* 108 (2015) 1–5.
- [169] K. Reuter, D. Frenkel, M. Scheffler, The steady state of heterogeneous catalysis, studied by first-principles statistical mechanics, *Phys. Rev. Lett.* 93 (2004) 116105.
- [170] J. Greeley, M. Mavrikakis, Alloy catalysts designed from first principles, *Nat. Mater.* 3 (2004) 810–815.
- [171] Y. Ji, H. Dong, T. Hou, Y. Li, Monolayer graphitic germanium carbide (g-GeC): the promising cathode catalyst for fuel cell and lithium-oxygen battery applications, *J. Mater. Chem. A* 6 (2018) 2212–2218.
- [172] A. Lee, D. Krishnamurthy, V. Viswanathan, Exploring MXenes as cathodes for non-aqueous lithium-oxygen batteries: design rules for selectively nucleating Li_2O_2 , *ChemSusChem* 11 (2018) 1911–1918.
- [173] M. Lee, Y. Hwang, K.-H. Yun, Y.-C. Chung, Cathode reaction mechanism on the h-BN/Ni (111) heterostructure for the lithium-oxygen battery, *J. Power Sources* 307 (2016) 379–384.
- [174] Y. Hwang, K.-H. Yun, Y.-C. Chung, Carbon-free and two-dimensional cathode structure based on silicene for lithium-oxygen batteries: a first-principles calculation, *J. Power Sources* 275 (2015) 32–37.
- [175] W. Zhang, L. Sun, J.M.V. Nsanzimana, X. Wang, Lithiation/delithiation synthesis of few layer silicene nanosheets for rechargeable Li-O_2 batteries, *Adv. Mater.* 30 (2018) e1705523.
- [176] L. Kavalsky, S. Mukherjee, C.V. Singh, Phosphorene as a catalyst for highly efficient nonaqueous Li-air batteries, *ACS Appl. Mater. Interfaces* 11 (2019) 499–510.
- [177] S. Wu, J. Yi, K. Zhu, S. Bai, Y. Liu, Y. Qiao, M. Ishida, H. Zhou, A super-hydrophobic quasi-solid electrolyte for Li-O_2 battery with improved safety and cycle life in humid atmosphere, *Adv. Energy Mater.* 7 (2017) 1601759.
- [178] H. Deng, Y. Qiao, S. Wu, F. Qiu, N. Zhang, P. He, H. Zhou, Nonaqueous, metal-free, and hybrid electrolyte Li-ion O_2 battery with a single-ion-conducting separator, *ACS Appl. Mater. Interfaces* 11 (2019) 4908–4914.
- [179] S. Chua, R. Fang, Z. Sun, M. Wu, Z. Gu, Y. Wang, J.N. Hart, N. Sharma, F. Li, D.-W. Wang, Hybrid solid polymer electrolytes with two-dimensional inorganic nanofillers, *Chem. A Eur. J.* 24 (2018) 18180–18203.
- [180] W.-K. Shin, A.G. Kannan, D.-W. Kim, Effective suppression of dendritic lithium growth using an ultrathin coating of nitrogen and sulfur codoped graphene nanosheets on polymer separator for lithium metal batteries, *ACS Appl. Mater. Interfaces* 7 (2015) 23700–23707.
- [181] J. Kumar, S.J. Rodrigues, B. Kumar, Interface-mediated electrochemical effects in lithium/polymer-ceramic cells, *J. Power Sources* 195 (2010) 327–334.
- [182] T. Yang, C. Shu, R. Zheng, A. Hu, Z. Hou, M. Li, Z. Ran, P. Hei, J. Long, Excellent electrolyte-electrode interface stability enabled by inhibition of anion mobility in hybrid gel polymer electrolyte based Li-O_2 batteries, *J. Membr. Sci.* 604 (2020) 118051.
- [183] S.J. Kang, T. Mori, J. Suk, D.W. Kim, Y. Kang, W. Wilcke, H.-C. Kim, Improved cycle efficiency of lithium metal electrodes in Li-O_2 batteries by a two-dimensionally ordered nanoporous separator, *J. Mater. Chem. A* 2 (2014) 9970–9974.
- [184] S.H. Park, T.H. Lee, Y.J. Lee, H.B. Park, Y.J. Lee, Graphene oxide sieving membrane for improved cycle life in high-efficiency redox-mediated Li-O_2 batteries, *Small* 14 (2018) 1801456.
- [185] L. Zhao, Y. Xing, X. Xie, J. Lai, N. Zhao, N. Chen, L. Li, F. Wu, R. Chen, Reducing the overpotential of an aprotic Li-O_2 battery using a conductive graphene interlayer, *Chem. Commun.* 55 (2019) 2102–2105.
- [186] J. Duan, W. Wu, A.M. Nolan, T. Wang, J. Wen, C. Hu, Y. Mo, W. Luo, Y. Huang, Lithium-graphite paste: an interface compatible anode for solid-state batteries, *Adv. Mater.* 31 (2019).
- [187] N.-W. Li, Y. Shi, Y.-X. Yin, X.-X. Zeng, J.-Y. Li, C.-J. Li, L.-J. Wan, R. Wen, Y.-G. Guo, A flexible solid electrolyte interphase layer for long-life lithium metal anodes, *Angew. Chem. Int. Ed.* 57 (2018) 1505–1509.
- [188] B. Liu, J.-G. Zhang, W. Xu, Advancing lithium metal batteries, *Joule* 2 (2018) 833–845.
- [189] C.P. Yang, Y.X. Yin, S.F. Zhang, N.W. Li, Y.G. Guo, Accommodating lithium into 3D current collectors with a submicron skeleton towards long-life lithium metal anodes, *Nat. Commun.* 6 (2015) 8058.
- [190] Z. Li, X. Li, L. Zhou, Z. Xiao, S. Zhou, X. Zhang, L. Li, L. Zhi, A synergistic strategy for stable lithium metal anodes using 3D fluorine-doped graphene shuttle-implanted porous carbon networks, *Nano Energy* 49 (2018) 179–185.
- [191] P. Tan, B. Chen, H. Xu, H. Zhang, W. Cai, M. Ni, M. Liu, Z. Shao, Flexible Zn- and Li-air batteries: recent advances, challenges, and future perspectives, *Energy Environ. Sci.* 10 (2017) 2056–2080.
- [192] Z. Liang, Q. Zou, Y. Wang, Y.-C. Lu, Recent progress in applying *in situ*/operando characterization techniques to probe the solid/liquid/gas interfaces of Li-O_2 batteries, *Small Methods* 1 (2017) 1700150.
- [193] E. Yoo, H. Zhou, Enhanced cycle stability of rechargeable Li-O_2 batteries by the synergy effect of a LiF protective layer on the Li and DMTFA additive, *ACS Appl. Mater. Interfaces* 9 (2017) 21307–21313.
- [194] J. Wang, J. Liu, Y. Cai, F. Cheng, Z. Niu, J. Chen, Super P carbon modified lithium anode for high-performance Li-O_2 batteries, *ChemElectroChem* 5 (2018) 1702–1707.
- [195] J. Yi, Y. Liu, Y. Qiao, P. He, H. Zhou, Boosting the cycle life of Li-O_2 batteries at elevated temperature by employing a hybrid polymer-ceramic solid electrolyte, *ACS Energy Lett.* 2 (2017) 1378–1384.
- [196] E. Peled, The electrochemical behavior of alkali and alkaline earth metals in non-aqueous battery systems—the solid electrolyte interphase model, *J. Electrochem. Soc.* 126 (1979) 2047–2051.
- [197] R. Zhang, N.W. Li, X.B. Cheng, Y.X. Yin, Q. Zhang, Y.G. Guo, Advanced micro/nanostructures for lithium metal anodes, *Adv. Sci.* 4 (2017) 1600445.
- [198] Z. Huang, J. Ren, W. Zhang, M. Xie, Y. Li, D. Sun, Y. Shen, Y. Huang, Protecting the Li-metal anode in a Li-O_2 battery by using boric acid as an SEI-forming additive, *Adv. Mater.* 30 (2018) e1803270.
- [199] Q.-C. Liu, J.-J. Xu, S. Yuan, Z.-W. Chang, D. Xu, Y.-B. Yin, L. Li, H.-X. Zhong, Y.-S. Jiang, J.-M. Yan, X.-B. Zhang, Artificial protection film on lithium metal anode toward long-cycle-life lithium-oxygen batteries, *Adv. Mater.* 27 (2015) 5241–5247.
- [200] R. Zhang, X.R. Chen, X. Chen, X.B. Cheng, X.Q. Zhang, C. Yan, Q. Zhang, Lithophilic sites in doped graphene guide uniform lithium nucleation for dendrite-free lithium metal anodes, *Angew. Chem. Int. Ed.* 56 (2017) 7764–7768.
- [201] X.-B. Cheng, H.J. Peng, J.-Q. Huang, R. Zhang, C.-Z. Zhao, Q. Zhang, Dual-phase lithium metal anode containing a polysulfide-induced solid electrolyte interphase and nanostructured graphene framework for lithium sulfur batteries, *ACS Nano* 9 (2015) 6373–6382.
- [202] H. Cheng, Y. Mao, J. Xie, Y. Lu, X. Zhao, Dendrite-free fluorinated graphene/lithium anodes enabling *in situ* LiI formation for high-performance lithium-oxygen cells, *ACS Appl. Mater. Interfaces* 11 (2019) 39737–39745.
- [203] W.-J. Kwak, S.-J. Park, H.-G. Jung, Y.-K. Sun, Optimized concentration of redox mediator and surface protection of Li metal for maintenance of high energy efficiency in Li-O_2 batteries, *Adv. Energy Mater.* 8 (2018) 1702258.
- [204] Y. Kim, D. Koo, S. Ha, S.C. Jung, T. Yim, H. Kim, S.K. Oh, D.M. Kim, A. Choi, Y. Kang, K.H. Ryu, M. Jang, Y.K. Han, S.M. Oh, K.T. Lee, Two-dimensional phosphorene-derived protective layers on a lithium metal anode for lithium-oxygen batteries, *ACS Nano* 12 (2018) 4419–4430.
- [205] D. Lin, Y. Liu, A. Pei, Y. Cui, Nanoscale perspective: materials designs and understandings in lithium metal anodes, *Nano Res.* 10 (2017) 4003–4026.
- [206] Y.S. Hong, C.Z. Zhao, Y. Xiao, R. Xu, J.J. Xu, J.Q. Huang, Q. Zhang, X. Yu, H. Li, Safe lithium-metal anodes for Li-O_2 batteries: from fundamental chemistry to advanced characterization and effective protection, *Batteries Supercaps* 2 (2019) 638–658.
- [207] G. Huang, J. Han, F. Zhang, Z. Wang, H. Kashani, K. Watanabe, M. Chen, Lithophilic 3D nanoporous nitrogen-doped graphene for dendrite-free and ultrahigh-rate lithium-metal anodes, *Adv. Mater.* 31 (2019) e1805334.
- [208] P. Albertus, S. Babinec, S. Litzelman, A. Newman, Status and challenges in enabling the lithium metal electrode for high-energy and low-cost rechargeable batteries, *Nat. Energy* 3 (2018) 16–21.
- [209] G. Huang, J. Han, C. Yang, Z. Wang, T. Fujita, A. Hirata, M. Chen, Graphene-based quasi-solid-state lithium-oxygen batteries with high energy efficiency and a long cycling lifetime, *NPG Asia Mater.* 10 (2018) 1037–1045.
- [210] A. Wang, S. Tang, D. Kong, S. Liu, K. Chiou, L. Zhi, J. Huang, Y.Y. Xia, J. Luo, Bending-tolerant anodes for lithium-metal batteries, *Adv. Mater.* 30 (2018) 703891.
- [211] Z. Guo, J. Li, Y. Xia, C. Chen, F. Wang, A.G. Tamirat, Y. Wang, Y. Xia, L. Wang, S. Feng, A flexible polymer-based Li-air battery using a reduced graphene oxide/Li composite anode, *J. Mater. Chem. A* 6 (2018) 6022–6032.
- [212] B. Hou, X. Lei, S. Zhong, B. Sun, C. Ouyang, Dissociation of $(\text{Li}_2\text{O}_2)^{0+}$ on graphene and boron-doped graphene: insights from first-principles calculations, *Phys. Chem. Chem. Phys.* 22 (2020) 14216–14224.
- [213] S.V. Pavlov, S.A. Kislenko, Investigation of the graphene-electrolyte interface in Li-air batteries: a molecular dynamics study, *J. Phys. Conf. Ser.* 946 (2018) 012028.
- [214] P. Wunderlich, J. Küpper, U. Simon, Anomalous discharge behavior of graphite nanosheet electrodes in lithium-oxygen batteries, *Materials* 13 (2020) 43.
- [215] F.S. Gittleson, K.P.C. Yao, D.G. Kwabi, S.Y. Sayed, W.-H. Ryu, Y. Shao-Horn, A.D. Taylor, Raman spectroscopy in lithium-oxygen battery systems, *Chemelectrochem* 2 (2015) 1446–1457.
- [216] H. Zheng, D. Xiao, X. Li, Y. Liu, Y. Wu, J. Wang, K. Jiang, C. Chen, L. Gu, X. Wei, Y.-S. Hu, Q. Chen, H. Li, New insight in understanding oxygen reduction and evolution in solid-state lithium oxygen batteries using an *in situ* environmental scanning electron microscope, *Nano Lett.* 14 (2014) 4245–4249.
- [217] L. Zhong, R.R. Mitchell, Y. Liu, B.M. Gallant, C.V. Thompson, J.Y. Huang, S.X. Mao, Y. Shao-Horn, *In situ* transmission electron microscopy observations of electrochemical oxidation of Li_2O_2 , *Nano Lett.* 13 (2013) 2209–2214.
- [218] R. Wen, M. Hong, H.R. Byon, *In situ* AFM imaging of Li-O_2 electrochemical reaction on highly oriented pyrolytic graphite with ether-based electrolyte, *J. Am. Chem. Soc.* 135 (2013) 10870–10876.
- [219] J. Wandt, P. Jakes, J. Granwehr, H.A. Gasteiger, R.-A. Eichel, Singlet oxygen formation during the charging process of an aprotic lithium-oxygen battery, *Angew. Chem. Int. Ed.* 55 (2016) 6892–6895.
- [220] S. Ganapathy, B.D. Adams, G. Stenou, M.S. Anastasaki, K. Goubitz, X.-F. Miao, L.F. Nazar, M. Wagemaker, Nature of Li_2O_2 oxidation in a Li-O_2 battery revealed by *operando* X-ray diffraction, *J. Am. Chem. Soc.* 136 (2014) 16335–16344.
- [221] Y.-C. Lu, E.J. Crumlin, G.M. Veith, J.R. Harding, E. Mutoro, L. Baggetto, N.J. Dudney, Z. Liu, Y. Shao-Horn, *In situ* ambient pressure X-ray photoelectron spectroscopy studies of lithium-oxygen redox reactions, *Sci. Rep.* 2 (2012) 715.
- [222] W. Xu, V.V. Viswanathan, D. Wang, S.A. Towne, J. Xiao, Z. Nie, D. Hu, J.-G. Zhang, Investigation on the charging process of Li_2O_2 -based air electrodes in Li-O_2 batteries with organic carbonate electrolytes, *J. Power Sources* 196 (2011) 3894–3899.
- [223] Y. Qiao, S. Ye, Spectroscopic investigation for oxygen reduction and evolution reactions with tetrathiafulvalene as a redox mediator in Li-O_2 battery, *J. Phy. Chem. C* 120 (2016) 15830–15845.
- [224] Q. Peng, J. Chen, H. Ji, A. Morita, S. Ye, Origin of the overpotential for the oxygen evolution reaction on a well-defined graphene electrode probed by *in situ* sum frequency generation vibrational spectroscopy, *J. Am. Chem. Soc.* 140 (2018) 15568–15571.

- [225] Peng Q, Y. Qiao, K. Kannari, A. Ge, K. Inoue, S. Ye, In situ spectroscopic investigations of electrochemical oxygen reduction and evolution reactions in cyclic carbonate electrolyte solutions, *J. Phys. Chem. C* (2020), doi:10.1021/acs.jpcc.0c03929.
- [226] J. Zheng, Q. Zhao, T. Tang, J. Yin, C.D. Quilty, G.D. Renderos, X. Liu, Y. Deng, L. Wang, D.C. Bock, C. Jaye, D. Zhang, E.S. Takeuchi, K.J. Takeuchi, A.C. Marschilok, L.A. Archer, Reversible epitaxial electrodeposition of metals in battery anodes, *Science* 366 (2019) 645–648.
- [227] S. Basak, J. Jansen, Y. Kabiri, H.W. Zandbergen, Towards optimization of experimental parameters for studying Li-O₂ battery discharge products in TEM using in situ EELS, *Ultramicroscopy* 188 (2018) 52–58.
- [228] X.-B. Han, K. Kannari, S. Ye, In situ surface-enhanced Raman spectroscopy in Li-O₂ battery research, *Curr. Opin. Electrochem.* 17 (2019) 174–183.
- [229] J. Wandt, P. Jakes, J. Granwehr, H.A. Gasteiger, R.-A. Eichel, Singlet oxygen formation during the charging process of an aprotic lithium-oxygen battery, *Angew. Chem. Int. Ed.* 55 (2016) 6892–6895.
- [230] Q. Zou, Y.C. Lu, Solvent-dictated lithium sulfur redox reactions: an operando UV-vis spectroscopic study, *J. Phys. Chem. Lett.* 7 (2016) 1518–1525.